Department of Electrical and Computer Engineering
North South University

Senior Project Design

Optical Pulling and Pushing Force for Dielectric, Chiral and Plasmonic nano particles

Name:	ID:
1. Mustafizur Rahman Rana	163 1517 043
2. Syeda Prioty Sultana	162 0138 043
3. Fabiha Rahman Efa	162 0981 043

Faculty Advisor:
Dr. Mahdy Rahman Chowdhury
Associate Professor
Department of Electrical and Computer Engineering
North South University
Fall 2020

Declaration

This is to declare that no part of this report or the project has been previously submitted elsewhere for the fulfillment of any other degree or program. Proper acknowledgement has been provided for any material that has been taken from previously published sources in the bibliography section of this report.

.....

Mustafizur Rahman Rana
Department of Electrical and Computer Engineering
North South University, Bangladesh

.....

Syeda Prioty Sultana
Department of Electrical and Computer Engineering
North South University, Bangladesh

.....

Fabiha Rahman Efa
Department of Electrical and Computer Engineering
North South University, Bangladesh

Approval

The Senior Design Project entitle “Optical Pulling and Pushing Force for Dielectric, Chiral and Plasmonic nano particles” by Mustafizur Rahman Rana, Syeda Prioty Sultana and Fabiha Rahman Efa has been accepted as satisfactory and approved for partial fulfillment of the requirement of BS in EEE degree program.

……

Supervisor’s Signature

Dr. Mahdy Rahman Chowdhury

Associate Professor

Department of Electrical and Computer Engineering

North South University

Dhaka, Bangladesh.

……

Dr. Mohammad Rezaul Bari

Associate Professor & Chair

Department of Electrical and Computer Engineering

North South University.

Dhaka, Bangladesh.

Acknowledgement

First of all, we would like to express our profound gratitude to our honorable course instructor, Dr. Mahdy Rahman Chowdhury, for his constant and meticulous supervision, valuable suggestions, his patience and encouragement to complete this research.

We would like to thank everybody who supported us and provided with guidance for the completion of this research.

Abstract

Optical pulling has been demonstrated on dielectric, plasmonic and chiral nanostructures using dielectric substrate. On the plasmonic substrate, the optical pushing force is also visible. For a specific wavelength range, optical pulling force can be obtained on a dielectric substrate. For estimating optical pulling force on nanostructures, we devised a general framework based on the time averaged Minkowski stress tensor. There is also a demonstration of a failed attempt to locate pulling force on a plasmonic substrate. The pulling force in dielectric particles on dielectric substrate is caused by the interference of electric quadrupole and dipole. The recoil force in a chiral particle can be used to create pulling force. The pulling force in plasmonic particles is caused by the current density.

Table of Contents

CHAPTER-1
INTRODUCTION

The optical regime of electromagnetic forces has been the source of numerous studies and, as a result, has received a lot of attention [1,2,48]. The oscillation of electric and magnetic fields produces electromagnetic waves. The electric and magnetic fields are perpendicular to the direction of the EM wave. Electromagnetic (EM) waves have momentum, and the quantum of light, photon, has a linear momentum of $\hbar\kappa$. Because light has momentum, the momentum exchange between light and particle will produce a force [3]. When light is scattered or absorbed in a single particle, the force can cause the particle to move; light can be used to control particle movement in this way. This force is called the optical force [4-6].

Optical manipulation based on optical gradient, scattering, and curl force by interacting light and matter has sparked a lot of interest in research disciplines [4,8]. The optical pulling force is the force that can draw an object in the direction of the source [3]. This intriguing phenomenon was first predicted in acoustics by Marston in 2006, and soon was extended to optics [9,10]. The use of a beam of light to pull a particle towards the source via a backward scattering effect, known as optical pulling force, is counterintuitive [8]. Pulling implies that the object travels in the opposite direction of light propagation (or that the force is reversed). However, in other circumstances, the "direction of light propagation" is unclear since the wavevector and Poynting vector directions may disagree, particularly in structured optical beams and nanostructures connected to optical pulling force.

Optical pulling is one of the most intriguing among the new manipulation freedoms, and it has also gotten a lot of attention because of the potential applications and the physics behind it [11-14]. When illuminated by a closely concentrated beam, the restoring force of the intensity gradient usually overcomes the scattering force, trapping the object around the focus spot. The intensity gradient force, on the other hand, vanishes when lit by an unfocused beam, and the item is predicted to be pushed away. According to a research found about 10 years ago, when illuminated by an unfocused beam, such as a diffraction-free (non diffraction) Bessel beam which is referred to as an optical tractor beam, the object may feel an optical pulling force (OPF) toward the source direction (OTB) [15-16].

Tractor beam is a recently popularized concept in the field of photon momentum transfer or optical force [17-19]. In contrast to the conventional pushing force, a tractor beam is a customized light beam that produces a counterintuitive negative force on a scatterer, dragging it in the opposite direction of light propagation [17-24]. Tractor beam experiments with a material background [20-22] can also be studied extensively to better understand the long-debated roles of various photon momenta [25].

Although it may appear counterintuitive, optical pulling force has recently been theoretically proven and experimentally demonstrated, as this paper will discuss. Marston in acoustics was the first to observe the pulling force of a single beam [26,27]. When he discovered that the axial radiation force of a Bessel acoustic beam on a sphere may be inverted (from pushing to pulling) for some well-built items, suppressing scattering to the back hemisphere. It's not surprising to find pulling force in optics using identical approaches because acoustic and optical waves share many similarities. In an optical solenoid beam, which is a diffraction less beam with in-plane intensity peak spirals around the optical axis, Lee anticipated optical pulling phenomena shortly after Marston. Sukhov and Dogariu validated the notion of optical tractor beam in the same year [28]. Following that, Chen and Novitsky independently produced two theoretical studies that provided a clear explanation of the criteria and procedure for obtaining an optical pulling force. Since then, the optical tractor beam has gotten a lot of attention because of the fascinating occurrences and physics involved, as well as the possible implications in optical manipulation technology. Furthermore, the optical tractor beam and pulling force concepts have been applied to various types of waves, such as water waves [29] and quantum matter waves [10].

We'd like to talk about the theoretical and numerical methodologies used to explore the optical pulling force before we go into the details of the optical pulling force. optical pulling force's computation methods are essentially identical to those employed in optical trapping [30]. The dipole approximation might be utilized to obtain analytical formulations for the optical forces from which the optical pulling force might be recognized for objects much smaller than the wavelength of the trapping light [30]. The direction of the optical force is determined in this case by the exceptional angular scattering properties of magnetic or bigger dielectric particles, and the Kerker scattering conditions are beneficial in studying the optical pulling force [30,33]. The ray tracing approach could be used to determine the optical forces for objects much larger than the wavelength [34,35]. To determine the optical force for objects of modest size similar to the wavelength, an integration of Maxwell's stress tensor on a closed surface surrounding the object is required [3]. The electromagnetic fields around the object are often obtained using numerical simulation methods such as the finite-difference time-domain approach or finite-element approaches. We will skip the detailed procedures because those can be found easily in the literature, and readers can refer to the references as needed.

In this article, we have investigated optical pulling force for dielectric, chiral and plasmonic nanoparticles using dielectric and plasmonic substrate. We aim to combine three nanoparticles (Chiral, dielectric and plasmonic) in a dielectric substrate and a plasmonic substrate using tractor beams in order to find the pulling force. We have shown a clear connection among the particles to obtain optical pulling force at specific wavelength range. As the particles were smaller than the wavelength, dipole approximation is used to explain both dielectric and chiral nanoparticles. To explain plasmonic nanoparticle we have used the Lorentz force. We have also discovered areas where optical pushing force dominated optical pulling force. Our investigation has focused on the contrast of dielectric and plasmonic substrates. Also, we have observed different behavior of optical force on three nanoparticles when the substrate is altered.

Previous works have demonstrated acting optical force on chiral, dielectric or plasmonic force individually. The works also focused on the wavelength, particle's size and radius etc. But our experiment is not only a new idea to put three nanoparticles together but also shades light to the different behavior for different substrates. Our findings may help to identify further connections about particle's behavior for optical manipulation.

PULLING FORCE

When light strikes a particle, it causes a forward scattering force, and some of the light's energy is absorbed by the particle, resulting in a backward force in the direction of light propagation. As the photons are carried backwards of a light by the particle, this backward or negative force is the pulling force of the particle.

Optical pulling force, often known as negative force, occurs when light strikes an object in the opposite direction of the incident light. Different mechanisms can be used to create optical pulling force. Light has the ability to carry momentum. Because of total momentum conservation, the force acting on the particle occasionally points in the opposite direction of the incident wave propagation.

Optical pulling force can be created by concurrent excitation of an electric dipole moment and a magnetic dipole moment or an electric quadrupole moment, resulting in intense forward scattering. The coupling of linear and angular momentums via chirality gives rise to a new mechanism for optical pulling force for chiral particles.

If an object can scatter incident light in a mode with low forward momentum to an outgoing mode with higher forward momentum, optical scattering force can generate a pulling force [36-40]. Crossed momentum shifts from linear to angular and creates optical pulling forces. The matter of dissipating optical forces by non-chiral and chiral contributions, as perfectly exposed by a circularly polarized plane wave, gives birth to optical pulling forces. Negative mechanical effect is the negative optical torque, where the electromagnetic field exerts torque on a particle in a direction opposite to its angular momentum [42,43]. Strong negative force components are formed by crossing transfers from the particle's optical angular momentum to linear momentum [41].

When incoming light falls on a particle, the recoil force is the force that is perpendicular to the scattered force. The recoil force originates from the coupling between the electric multipoles of adjacent orders of the poles. The value of recoil force is determined by the fraction of the extinction coefficient induced by electric and magnetic dipoles, as well as their cross product [44] The rearward force, also known as an optical pulling force or a negative scattering force, is caused by the recoil force of scattered photons from the chiral particle's illumination [45]. In the formula for a non-chiral particle, there are no chirality dependent terms [46,47].

An optical tractor beam is a light beam that can draw an item toward the source direction by exerting an optical pulling force (OPF). When illuminated by an unfocused beam such as a diffraction-free (nondiffracting) Bessel beam, also known as an optical tractor beam, an optical pulling force (OPF) toward the source direction can be achieved (OTB).

According to the rule of conservation of momentum, shooting light towards an object with the momentum of the light will drive the object away from the light source. If the light impacts the object and the light acquires forward motion rather than losing it, the object will lose momentum in the forward direction, even to the point of traveling backwards and towards the light source, according to the law of conservation of momentum. So, there's a technique to construct a tractor beam that doesn't break the laws of physics. We got a backward push towards light propagation in our experiment. So, in our experiment, light loses some of its forward speed after colliding with it, resulting in backward scattering force, also known as pulling force.

CHAPTER-2
OPTICAL SETUP AND METHOD

In this paper, we have investigated nanoparticles' activity (plasmonic, dielectric, and chiral) in the air medium. Positioning a plasmonic, dielectric, and chiral particles are positioned over a dielectric substrate, we have demonstrated a general method for determining optical pulling force. Our proposed configuration provides a standardized mechanism for determining visual pulling force for three nanoparticles (plasmonic, dielectric, and chiral), which can be confirmed using a simple experimental setup. The nanoparticles are (plasmonic, dielectric, chiral) positioned with the dielectric substrate, as shown in a schematic diagram of our proposed simple setup in figure (a). The dielectric nanoparticle is placed in the center of the surface as shown as in figure (a), the chiral nanoparticle is placed on the left side of the dielectric nanoparticle and the plasmonic nanoparticle is placed on the right side of it. The radius of three nanoparticles (plasmonic, dielectric, chiral) is 100 nm (r = 100 nm), and the distance between each particle is also 100 nm (d = 100 nm). In this article, the wavelength (lambda) is varied from 440 nm to 1200 nm. In this experiment, two plane beam is used and the equation is $\mathrm{E} = [\mathrm{E}_{\circ}\, \mathrm{e}^{\mathrm{jkz}} + \mathrm{E}_{\circ}\mathrm{e}^{-\mathrm{jk}(\mathrm{xcos}\theta - \mathrm{zsin}\theta)}]\hat{\mathrm{Y}}$. One incident beam propagates ''-z'' axis and is polarized electric field along the y axis. In contrast, another incident beam propagates ''+x'' axis with an angle of 20 degrees (theta= 20) and is polarized Electric field along the y axis. For chiral nanoparticle a silica based left-handed chiral nanoparticle (K = -1) is used. For the chirality parameter K = -1, the refractive index is 1.45.

The dielectric substrate has the following dimensions: width = 850 nm, depth = 1050 nm, and height = 400 nm. Nanoparticles are 7 nm (h=7 nm) away from the substrate in this experiment.

Figure (b) shows nanoparticles with plasmonic substrate (plasmonic, dielectric, and chiral). For more details, the dielectric nanoparticle is placed in the center of the surface, the chiral nanoparticle is placed on the left side of the dielectric nanoparticle and the plasmonic nanoparticle is placed on the right side of it. The radius of three nanoparticles (plasmonic, dielectric, chiral) is 100 nm (r = 100 nm), and the distance between each particle is also 100 nm (d = 100 nm). In this article, the wavelength (lambda) is varied from 440 nm to 1200 nm. In this experiment, two plane beam is used and the equation is $\mathrm{E} = [\mathrm{E}_{\circ}\, \mathrm{e}^{\mathrm{jkz}} + \mathrm{E}_{\circ}\mathrm{e}^{-\mathrm{jk}(\mathrm{xcos}\theta - \mathrm{zsin}\theta)}]\hat{\mathrm{Y}}$. One incident beam propagates ''-z'' axis and is polarized Electric field along the y axis. Another incident beam propagates ''+x'' axis with an angle of 20 degrees (theta= 20) and is polarized Electric field along the y axis. For chiral nanoparticle a silica based left-handed chiral nanoparticle (K = -1) is used. For the chirality parameter K = -1, the refractive index is 1.45.

The plasmonic substrate has the following dimensions: width = 850 nm, depth = 1050 nm, and height = 200 nm. Nanoparticles are 7 nm (h=7 nm) away from the substrate in this experiment.

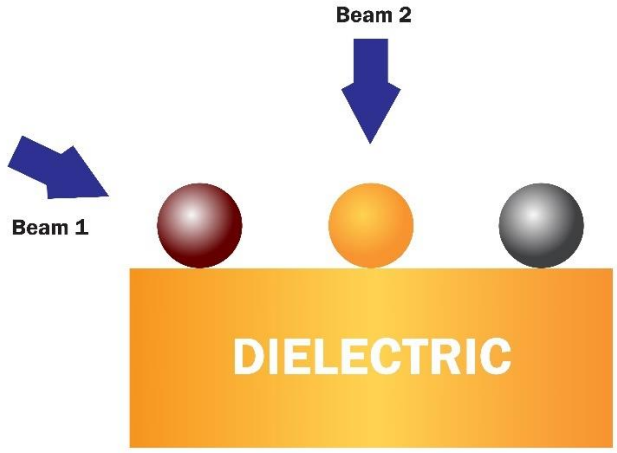

a

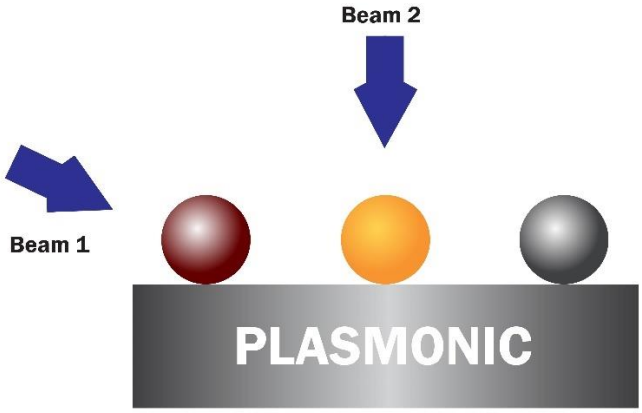

b

Figure 1 (a) and (b) presents the experimental demonstration of OPF by a dielectric substrate and plasmonic substrate. Three nanoparticles (chiral, dielectric and plasmonic) are equally placed 100 nm intermolecular distance apart from each other.

METHOD

The left side nanoparticle is referred to as nanoparticle 1, the middle nanoparticle as nanoparticle 2, and the exemplary side nanoparticle as nanoparticle 3. The optical forces measured outside the volume of these nanoparticles have been classified as exterior or outside optical forces in full-wave simulations using COMSOL Multiphysics. The outside visual force is measured using the background fields of the scatterer radius a and the time-averaged Minkowski stress tensor at r=a+ [48-52].

$$(F_{Total}^{out}) = \int (\bar{\bar{T}}^{out}) \,.\, d\boldsymbol{s}$$

$$< \bar{\bar{\boldsymbol{T}}}^{out} > = \frac{1}{2} Re\,[\boldsymbol{D}^{out}\, \boldsymbol{E}_{out}^{*} + \boldsymbol{B}^{out}\, \boldsymbol{H}_{out}^{*} - \frac{1}{2} \bar{\bar{\boldsymbol{I}}}\, (\boldsymbol{E}_{out}^{*} \,.\, \boldsymbol{D}_{out} + \boldsymbol{E}_{out}^{*} \,.\, \boldsymbol{B}_{out})]$$

Where 'out' denotes the scatterer's complete exterior area (incident field plus dispersed field); The electric field, displacement vector, magnetic field, and induction magnetic field vectors are represented by **E, D, H**, and **B**, respectively. The time average is represented by, and $\boldsymbol{I}$ mean, the unity tensor.

For the chiral object, the constitutive relations are given by [53-54]

$$\boldsymbol{D} = \boldsymbol{\varepsilon_0 \varepsilon E} + \boldsymbol{iK}\sqrt{\varepsilon_0 \boldsymbol{\mu}_0}\, \boldsymbol{H}$$

$$\boldsymbol{B} = \boldsymbol{\mu_0 \mu E} + \boldsymbol{iK}\sqrt{\varepsilon_0 \boldsymbol{\mu}_0}\, \boldsymbol{H}$$

Here, ε and μ are the relative permittivity and permeability of the chiral material respectively; k denotes the chirality parameter, which is controlled by the inequality k^2 < εμ [54]; and, finally, ε0 and μ0 are the permittivity and permeability in a vacuum. For the real and imaginary parts of the permittivity of Dielectric and plasmonic substrates have been taken from the standard Palik data [55].

MAXWELL STRESS TENSOR

Maxwell stress tensor is used to calculate electromagnetic force. Maxwell stress tensor is applied for linear and nonlinear conditions. It refers to the interaction between electromagnetic forces and mechanical momentum. A freely moving point charge's force can be calculated by Lorentz force law but in a complicated situation, tensor arithmetic is more convenient to compute. To calculate maxwell stress tensor, the electromagnetic force on the charges in volume v:

$$F = \int_v (E + v \times B)\rho d\tau = \int_v (\rho E + J \times B) d\tau$$

The force per unit volume:

$$f = \rho E + J \times B$$

Eliminating ρ and J by using maxwell's equation:

$$f = \epsilon_0 (\nabla \cdot E)E + \left(\frac{1}{\mu_0} \nabla \times B - \epsilon_0 \frac{dE}{dt}\right) \times B$$

$$\frac{d}{dt}(E \times B) = \left(\frac{dE}{dt} \times B\right) + \left(E \times \frac{dB}{dt}\right)$$

From faraday's law

$$\frac{dB}{dt} = -\nabla \times E$$

$$-\frac{dE}{dt} \times B = \frac{d}{dt}(E \times B) + E \times (\nabla \times E)$$

Thus,

$$f = \epsilon_0[(\nabla \cdot E)E - E \times (\nabla \times E)] - \frac{1}{\mu_0}[B \times (\nabla \times B)] - \epsilon_0 \frac{d}{dt}(E \times B)$$

since $\nabla \cdot B = 0$

To make things looks more symmetrical, let's throw in a term $(\nabla \cdot B)$ B; costs us nothing.

Meanwhile product rule four is,

$$\nabla(E^2) = 2(E \cdot \nabla)E + 2E \times (\nabla \times E)$$

So,

$$E \times (\nabla \times E) = \frac{1}{2}\nabla(E^2) - (E \cdot \nabla)E$$

We can write same for B. Therefore,

$$f = \varepsilon_0[(\nabla \cdot E)E + (E \cdot \nabla)E] + \frac{1}{\mu_0}[(\nabla \cdot B)B + (B \cdot \nabla)B] - \frac{1}{2}\nabla(\varepsilon_0 E^2 + \frac{1}{\mu_0}B^2) - \varepsilon_0 \frac{\delta}{\delta t}(E \times B)$$

simplifying the equation introducing the Maxwell stress tensor,

$$T_{ij} = \varepsilon_0(E_i E_j - \frac{1}{2}\delta_{ij}E^2) + \frac{1}{\mu_0}(B_i B_j - \frac{1}{2}\delta_{ij}B^2)$$

I and j refer coordinate x, y and z, so there are nine components (T_{xx} , T_{yy} , T_{xz} , T_{yx} and so on). The Kronecker delta, δ_{ij}, is 1 if the indices are the same ($\delta_{xx} = \delta_{yy} = \delta_{zz} = 1$) and zero otherwise ($\delta_{xy} = \delta_{xz} = \delta_{yz} = 0$). Thus

$$T_{xx} = \frac{1}{2}\varepsilon_0(E^2{}_x - E^2{}_y - E^2{}_z) + \frac{1}{2\mu_0}(B^2{}_x - B^2{}_y - B^2{}_z)$$

$$T_{xy} = \varepsilon_0(E_x E_y) + \frac{1}{\mu_0}(B_x B_y)$$

And so on.

Dot product of $\overleftrightarrow{T}$ can be formed with vector a in two ways:

$$(a \cdot \overleftrightarrow{T})_j = \sum_{i=x,y,z} a_i T_{ij}, \quad (\overleftrightarrow{T} \cdot a) = \sum_{i=x,y,z} T_{ji} a_i$$

The divergence of $\overleftrightarrow{T}$ is:

$$(\nabla \cdot \overleftrightarrow{T})_J = \varepsilon_0[(\nabla \cdot E)E_j + (E \cdot \nabla)E_j - \frac{1}{2} \nabla_j E^2] + \frac{1}{\mu_0}[(\nabla \cdot B)B + (B \cdot \nabla)B_j - \frac{1}{2} \nabla_j B^2]$$

So, force per unit volume is:

$$f = \nabla \cdot \overleftrightarrow{T} - \varepsilon_0 \mu_0 \frac{\delta S}{\delta t};$$ S is the pointing vector.

So, the total electromagnetic force on the charges v:

$$F = \oint_S \overleftrightarrow{T} \cdot da - \varepsilon_0 \mu_0 \frac{d}{dt} \int_V S d\tau$$

On static case:

$$F = \oint_S \overleftrightarrow{T} \cdot da$$

Here, $\overleftrightarrow{T}$ is the force in per unit area acting on the surface. The diagonal elements (T_{xx}, T_{yy}, T_{zz}) represent pressure and the off-diagonal elements (T_{xy}, T_{yz}, T_{zx}) represent shear terms.

CHAPTER-3
DIELECTRIC PARTICLE

Dielectrics are insulators. They are very poor conductors of electric current because of the nonexistence of any free electron. Also, there is no loosely bound electron exists which cancel out the chance off drifting electrons out of the dielectric material.

We can divide dielectric materials into two types; polar substance and nonpolar substance. H_2O (water) and NH_3 are the examples of polar substances. CO_2 (Carbon dioxide) and CH_4 (Methane) are the examples of nonpolar substances.

Dielectric materials can be polarized with the help of an external electric field. If the dielectric material is polarized, optical force is displayed [56].

In our experiment dielectric particles give us optical pulling force. In a uniform electric field, the net force of dielectric must be zero. Because the sum of forces on each dipole is zero. But, in a non-uniform electric field, a net force is present on each pole due to a different electric field. So, the particle will be pulled towards the region of increasing electric field.

To illustrate, if a dielectric is placed at the edge of parallel plate, which have been charged by opposite charges, the non-uniformity of the field at the edge will tend to pull the dielectric.

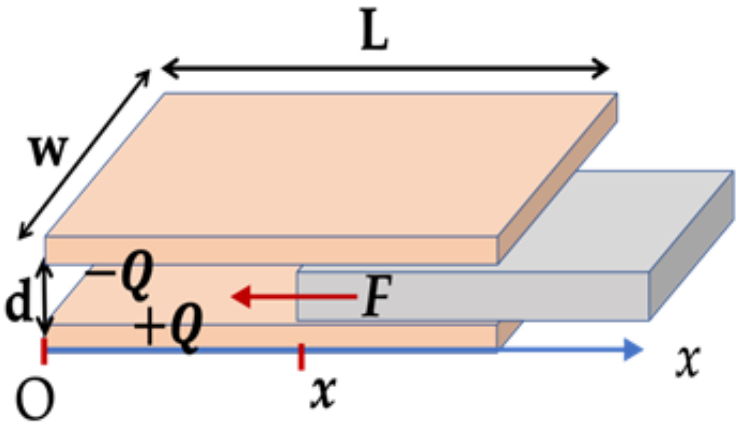

Put ±Q are on the plates separated by a distance d. Let w be the widths of the plate and L the length, and at some instant, let L −x along the length have a dielectric of dielectric constant ϵr and length x be empty. The force is given with the negative axis x.

$$F_x = -1/2\,(Q^2\, d/\epsilon_o\, w) \cdot (\epsilon r - 1)/[x+\epsilon r\,(L-x)]^2 \qquad (01)$$

The following plot shows that when the entire dielectric is just outside the edge, force is greatest, and as the dielectric gets pulled in further and further, the force decreases to zero when the dielectric is all the way in, which is at x=0x=0 in the plot.

In this experiment, we have obtained the pulling force of a dielectric particle using a dielectric substrate and compared it using a pec substrate. At the radius (r = 100 nm) of dielectric particles, early pulling force is obtained when the wavelength reaches 440 nm. The pulling force is acquired continuously with the increasing wavelength till 1200 nm.

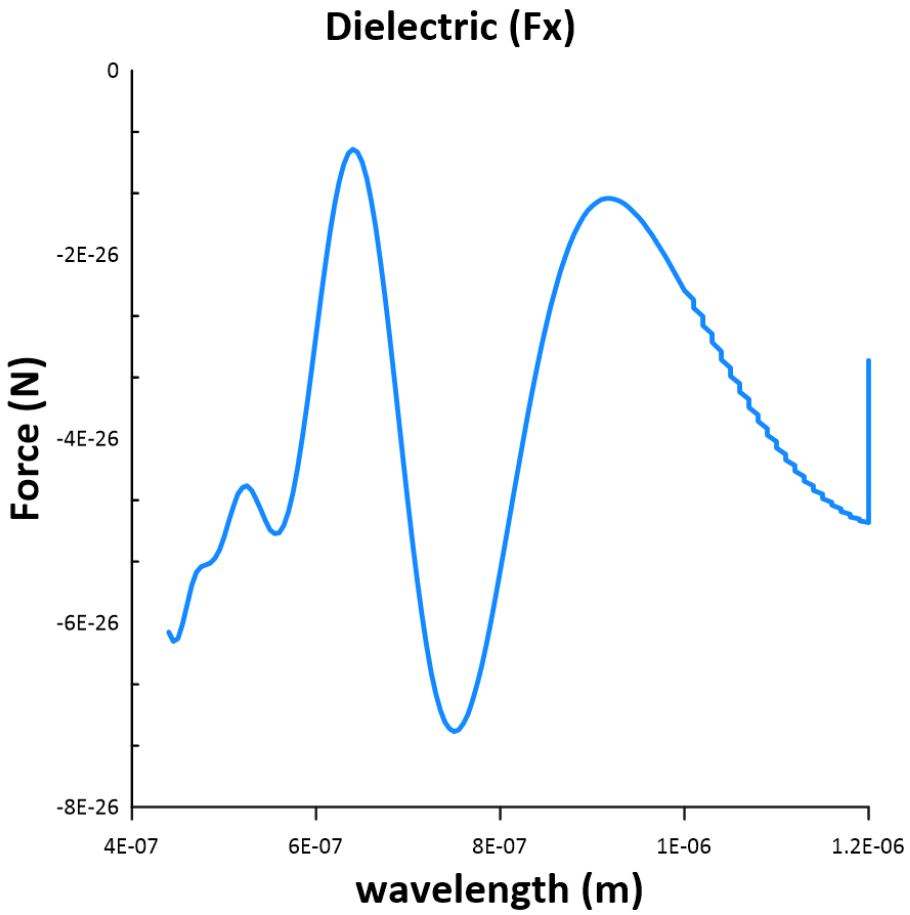

Figure 2 (a) presents the existence of optical pulling force to the x axis of the dielectric particle on the dielectric substrate from the wavelength of 440 nm to 1200 nm. From the graph, the highest optical pulling force wavelength range is shown between 700 nm to 800 nm.

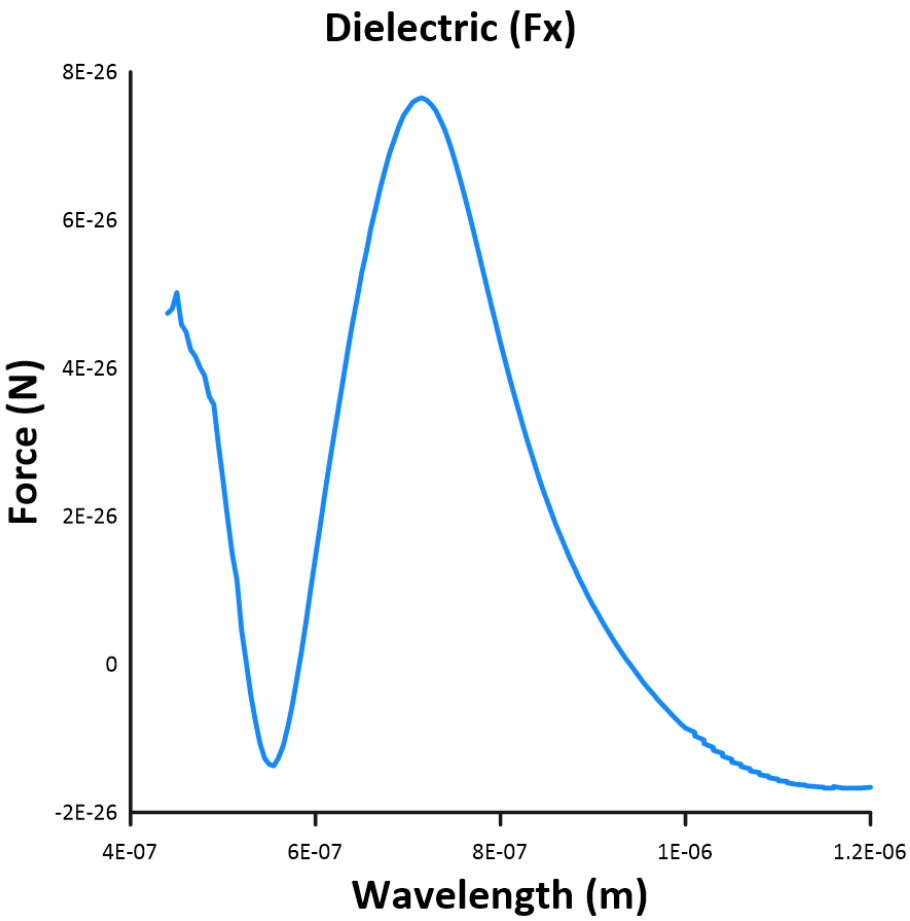

Figure 2 (b) represents optical pulling and pushing force of the dielectric particle toward the x axis on a plasmonic substrate. From the range of wavelength 530 nm to 580 nm and 945 nm to 1200 nm we have obtained pulling force. Also, we have got pushing force from 440 nm to 530 nm and 585 nm to 935nm.

The optical forces functioning on dielectric spherical particles can be calculated by Minkowski Stress Tensor method. We see that the force is negative and thus we ensure the existence of OPF. As large particles absorb more photons, the possibility of obtaining OPF is disintegrated. Transverse stability is the must have.

Here we will analyze the presence of OPF. The total induced time averaged optical force can be computed by integrating time averaged Minkowski stress tensor over a closed surface enclosing the particle [52].

$$\mathrm{F} = \oint_S \langle \boldsymbol{T} \rangle \cdot d\boldsymbol{s}$$

Here,

$$\langle \boldsymbol{T} \rangle = 1/2 \,\mathrm{Re}\,[\boldsymbol{D} \otimes \boldsymbol{E}* + \boldsymbol{B} \otimes \boldsymbol{H}* - 1/2\, I(\boldsymbol{E}* \cdot \boldsymbol{D} + \boldsymbol{H}* \cdot \boldsymbol{B})]$$

Where I is the identity matrix. With regard to the induced electric quadrupole order:

Suppose in free space, the time average optical force on a dielectric particle in a monochromatic optical field could be calculated by Eq. (2) by taking account of induced multipoles up to electric quadrupole.[76]

$$(F) = F_p + F_m + F_{Qe} + F_{pm} + F_{Qep} + \ldots \qquad (02)$$

$$= \frac{1}{2} Re\,[(\nabla E^*) \cdot p\,] + \frac{1}{2} Re\,[(\nabla B^*) \cdot m\,] + \frac{1}{4} Re\,[(\nabla\nabla E^*) : Q_e\,] - \frac{k^4}{12\pi\varepsilon_0 c} Re\,[p \times m^*\,] - \frac{k^5}{12\pi\varepsilon_0} Re\,[Q_e \times p^*\,] + \ldots$$

Let us express the time-averaged optical force on a conventional dielectric particle in terms of the induced multiples up to electric quadrupole order [58-60].

$$F = F_{incident} + F_{interference}$$

Where,

$$F_{incident} = F_p + F_m + F_{Qe} + \ldots$$

$$F_{interference} = F_{pm} + F_{Qep} + \ldots$$

Also,

$$F_p = \frac{1}{2} Re\,[(\nabla E^*) \cdot p]$$

$$F_m = \frac{1}{2} Re\,[(\nabla B^*) \cdot m]$$

$$F_{Qe} = \frac{1}{4} Re\,[(\nabla\nabla E^*) : Q_e\,]$$

$$F_{pm} = -\frac{k^4}{12\pi\varepsilon_0 c} Re\,[p \times m^*\,]$$

$$F_{Qep} = -\frac{k^5}{12\pi\varepsilon_0} Re\,[Q_e\, x p^*\,]$$

E and H are the incident electric and magnetic field vectors. $P = \alpha_e E$, $m = \alpha_m H$, $Q_e = (\gamma_e / 2)(\nabla E + \nabla E^T)$ are the induced electric dipole, magnetic dipole and electric quadrupole momentum respectively $\alpha_e = i6\pi\, \varepsilon_o\, a_1/k^3$, $\alpha_m = i6\pi\, b_1/k^3\mu_0$, $\gamma_e = i40\pi\varepsilon_0\, a_2/k^5$ are complex polarizabilities, $a1$, $b1$ and $a2$ are the Mie coefficients and k is the wave vector. The five terms in (2) are the contributions from electric dipole, magnetic dipole, electric quadrupole, electric–magnetic dipole interference and electric dipole–quadrupole interference respectively [52].

$F_{incident}$ is the multiplication of multi pole and incident field of field gradience. They represent the momentum removed by the particle, which is positive definite. $F_{incident}$ is the responsible force for optical pushing force. Accordingly, any negative force must be coming from $F_{interference}$. Every term in $F_{interference}$ is the product of two multipoles, which represent the recoil force induced by the interference of the field-excited multipole radiation. For appropriate phases in the multipoles, the interference may cause the particle to emit light forward resulting in a large recoil force that overcomes $F_{incident}$ (OPF) and results in pulling force.

In our setup, the dipole and quadrupole interference create an imbalance which works as the source of optical pulling force in dielectric particles. The imbalance has been created because the $F_{interference}$ is larger than $F_{incident}$. Hence the $F_{interference}$ is the responsible force of the required pulling force. As the tractor beam excites the multipoles, the optical pulling force is found by the interference enhanced forward scattering [8].

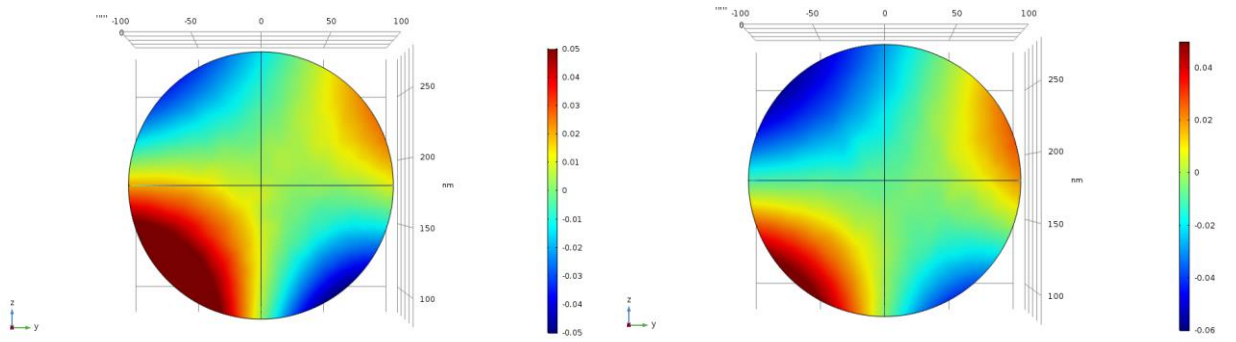

Figure 3 (a) presents the interference pattern of the electric dipole and quadrupole at 720 nm and 750 nm generated by the dielectric sub on the dielectric particle to the electric field x component. The expected interference creates an interaction of quadrupole where two larger poles and two smaller poles are produced.

To strengthen our founding, we are comparing plasmonic substrates in the same set up. But in the range of 720 and 750 nm of wavelength, dipoles are created in dielectric particles. We obtain optical pushing force instead of pulling force. The ground for this staggering optical force is

equation (2). Increasing the wavelength to 1000 nm, the dipole and quadrupole interference occurs and we manage to acquire pulling force in the plasmonic substrate. Note that, the finding's significance implies that $F_{incident}$ is the responsible force for pulling force in both dielectric and plasmonic substrate.

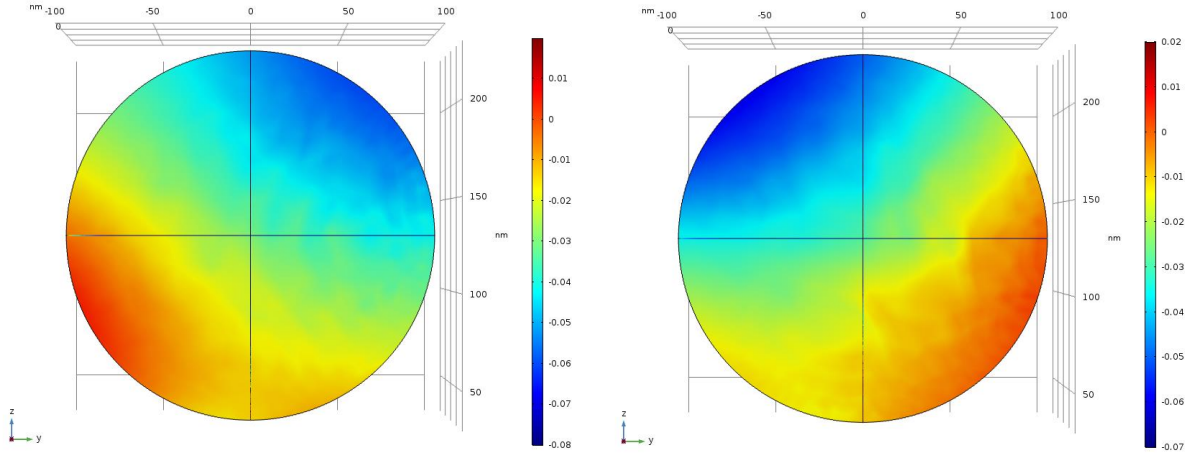

Figure 3 (b) represents the incident of electric dipoles at 720 nm and 750 nm generated by plasmonic substrate on the dielectric particle to the electric field x component.

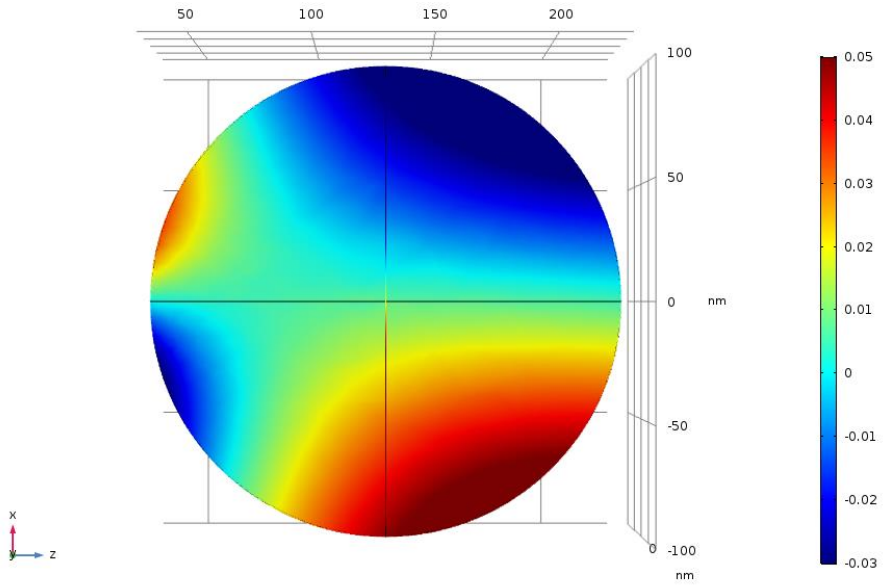

Figure 3 (c) presents the interference pattern of the electric dipole and quadrupole at 1000 nm generated by the plasmonic substrate on the dielectric particle to the electric field z component. The interference creates the same interaction pattern as dielectric substrate of quadrupole and two larger poles and two smaller poles are produced.

CHAPTER-4

CHIRAL PARTICLE

A chiral behavior differs from its mirrored counterpart. The tendency of a particle's spin to utilize either the right or left hand more naturally than the other is referred to as helicity (the projection of the spin onto the direction of momentum), which in the case of a minuscule massless particle is referred to as chirality. When the helicity of a particle is positive then it's right-handed when the direction of its spin is the same as the direction of its motion. The helicity of a particle is negative left-handed when the directions of spin and motion are opposite and for a standard clock, its spin vector is defined by the rotation of its hands. Left-handed helicity occurs if tossed with its directed forwards face.
Mathematically, helicity is the sign of the projection of the spin vector onto the momentum vector so we can say positive for right-handed and negative for left-handed.

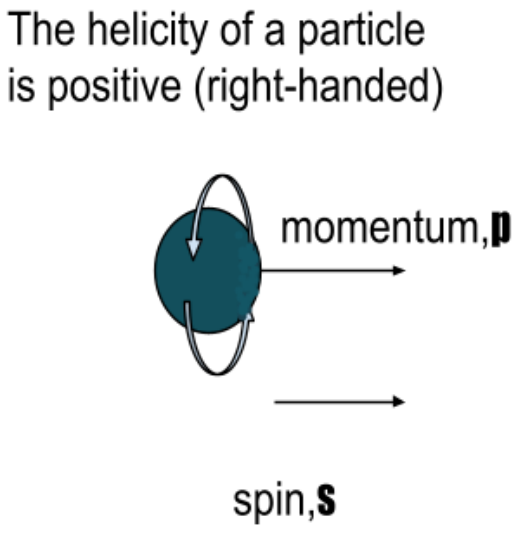

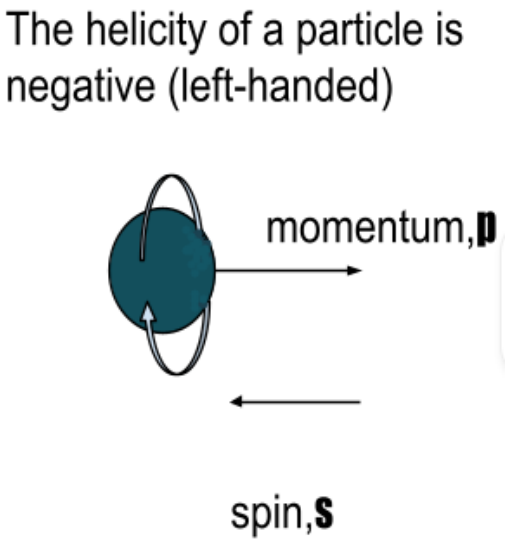

The chirality of a particle is determined by whether the particle transforms in a right- or left-handed. So, we can say a chiral particle is one whose mirror image cannot overlay on the original particle and the chirality of a particle is illuminated when it interacts with another chiral entity. In a Chirality expression, Chirality dependent terms should be calculated for the optical force acts on a chiral particle. Electromagnetic waves and monochromatic wave have chiral character, monochromatic wave chirality can be written as: [7,31,32].

The left and right circularly polarized plane waves interact with a chiral particle in a different way for their opposite chirality. So, we can say we can get different opposite optical forces. The chirality of a particle allows light to attract a chiral particle [4].

In this experiment, we are obtaining optical pulling force targeting chiral nanoparticle on dielectric substrate. Here, optical pulling force is acquired in the range of wavelength 535 nm to 565 nm and 645 nm to 1200 nm. In this setup, the highest pulling force range for dielectric sub is obtained at 700 nm to 800 nm.

Also, having the same set up, replacing dielectric substrate with plasmonic, we have observed optical pulling force in 1115 nm to 1200 nm wavelength.

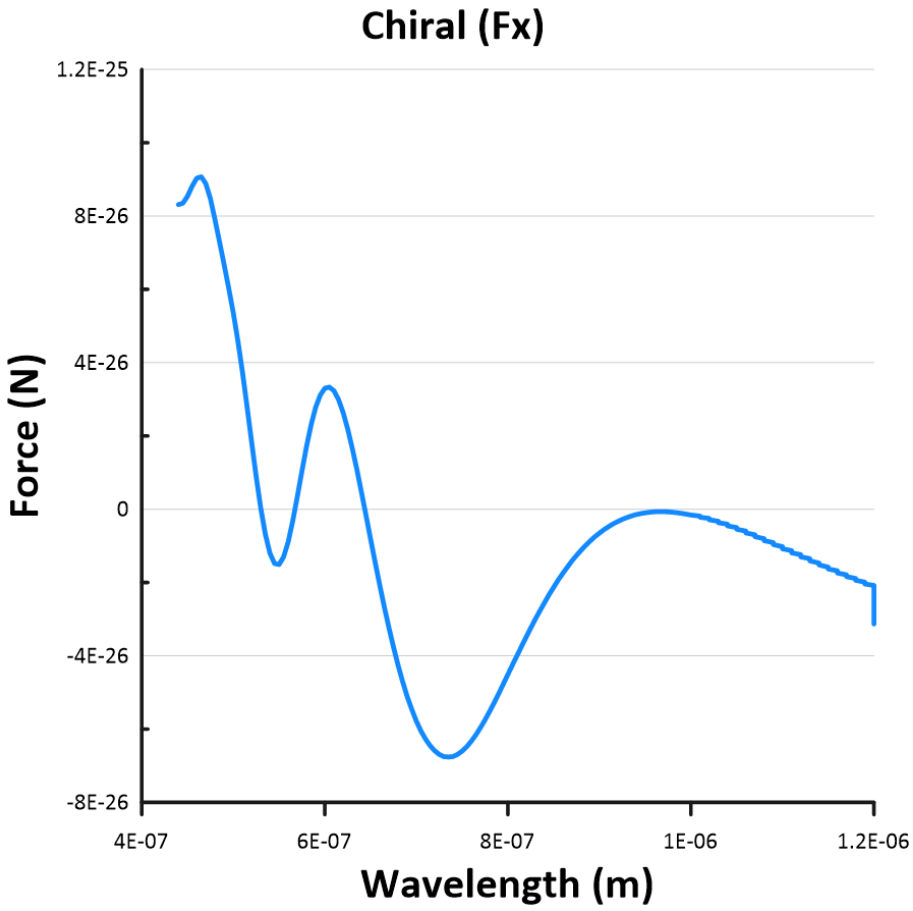

Figure 4 (a) presents the existence of optical pulling force to the x axis of the chiral particle on the dielectric substrate from the wavelength of 535 nm to 565 nm and also from the wavelength 645 nm to 1200 nm. From the graph, the highest optical pulling force wavelength range is shown between 700 nm to 800 nm

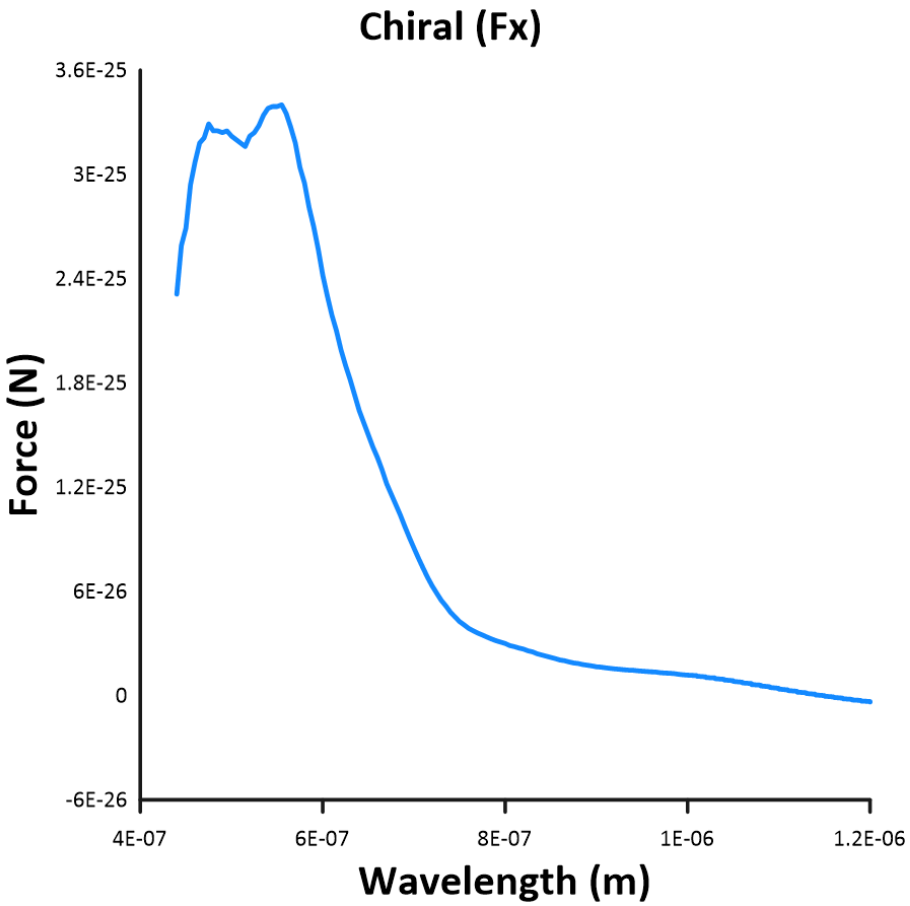

Figure 4 (b) represents optical pushing and pulling force of the chiral particle toward the x axis on a plasmonic substrate. From the range of wavelength 440 nm to 1145 nm we have got pushing force also we have obtained pulling force from wavelength 1150 nm to 1200 nm.

From the study of Chiral particle behavior, we have seen chirality dependent terms that couple mechanical linear momentum and optical angular momentum. Hence, the chirality induced coupling could be used as a possible way to obtain optical pulling force.

To demonstrate the physics, considering a tiny chiral particle with an induced electric dipole moment p and a magnetic dipole moment m, [61].

(Electric dipole moment),

$$p = \overleftrightarrow{\alpha}^{ee} E + \overleftrightarrow{\alpha}^{em} B$$

(Magnetic dipole moment),

$$m = -\overleftrightarrow{a}^{emT} E + \overleftrightarrow{a}^{mm} B$$

Here,

$\overleftrightarrow{a}^{ee}$ is the electric polarization tensor

$\overleftrightarrow{a}^{mm}$ is the magnetic polarization tensor

$\overleftrightarrow{a}^{em}$ is the chiral polarization tensor

$\overleftrightarrow{a}^{emT}$ is the transpose of chiral polarization tensor

A^T designates the transpose of A. The explanation can be done by using the dipole approximation regime as our incident wavelength is larger than the particle. Using Minkowski stress tensor, we can compute optical force on an object;

$$\langle F \rangle = \frac{1}{8\pi} Re\{ \oiint_s \left[\varepsilon (E \cdot s) E^* + \mu^{-1} (B \cdot s) B^* - \frac{1}{2} (\varepsilon |E|^2 + \mu^{-1} |B|^2) s \right] dS \} \quad (03)$$

Here E and B are the incident and scattered fields where,

$$E = E_i + E_s$$

$$B = B_i + B_s$$

The equation (3) can be reduced to

$$\langle F \rangle = \frac{1}{2} Re\{ p(\nabla \otimes E_I^*) + m(\nabla \otimes B_I^*) - \frac{2k^4}{3} \sqrt{\frac{\mu}{\varepsilon}} (p \times m^*) \} \quad (04)$$

For having linear case, the electric and magnetic dipole moments are proportional to the incident field,

$$P = \alpha_e E \quad and \quad m = \alpha_m H$$

where the two complex polarizabilities are $\alpha_i = \frac{3i\varepsilon a_1}{2k^3}$ *and* $\alpha_m = \frac{3ib_1}{2\mu k^3}$

Here, a_1 and b_2 are Mie coefficients.

So, after some mathematical operation, the total time-averaged optical force of Eq. (4) can be expressed in terms of the polarizabilities [62].

$$(F) = (F_e) + (F_m) + (F_{e-m})$$

Where electric dipole force is,

$$(F_e) = ¼\, Re(\alpha_e)\nabla|E|^2 + \frac{k}{2n} Im(\alpha_e) Re(E \times B^*) + \frac{1}{2} Im(\alpha_e) Im[(E^* \cdot \nabla)E]$$

The magnetic dipole force is,

$$(F_m) = ¼\, Re(\alpha_m)\nabla|B|^2 + \frac{k}{2n} Im(\alpha_m) Re(E \times B^*) + \frac{1}{2} Im(\alpha_m) Im[(B^* \cdot \nabla)B]$$

And the recoil force is

$$(F_{e-m}) = -\frac{k^4}{3}\sqrt{\frac{\mu}{\varepsilon}}[Re(\alpha_e \alpha_m^*) Re(E \times B^*) - Im(\alpha_e \alpha_m^*) Im(E \times B^*)] \quad (05)$$

$$= -\frac{k^4}{3}\sqrt{\frac{\mu}{\varepsilon}} Re(\alpha_e \alpha_m^*) Re(E \times B^*) - \frac{k^3}{3}\mu\, Im(\alpha_e \alpha_m^*) \times \{½\, \nabla|E|^2 - Re[(E^* \cdot \nabla)E]\}$$

The recoil force, responsible for pulling force, resulting from the interaction of electric and magnetic dipole moment also contributes to the intensity gradient force and scattering force.

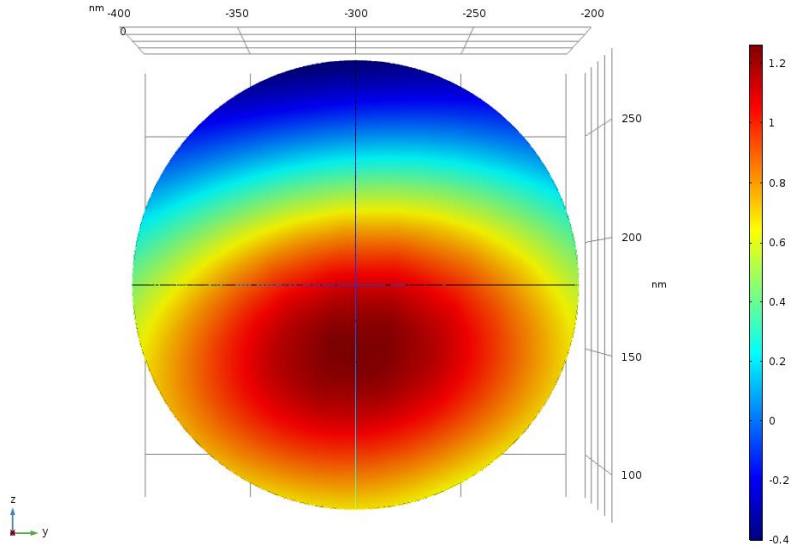

a

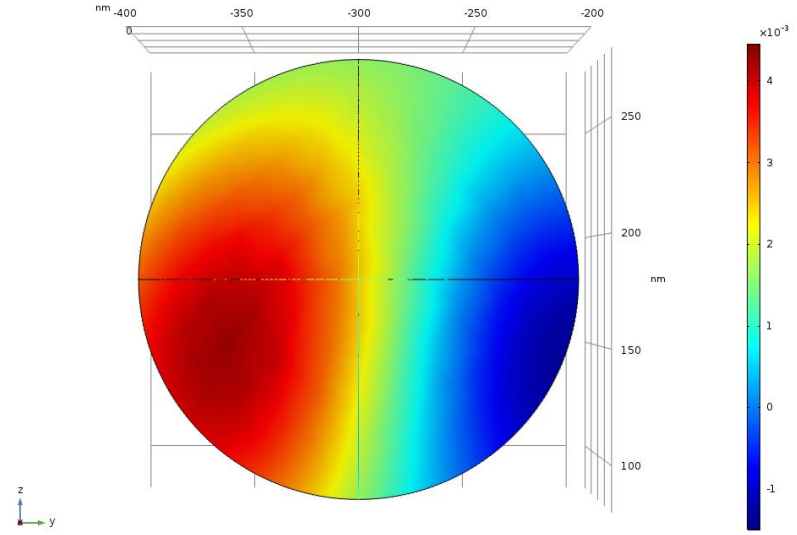

b

Figure 5 (a) represents electric dipole at 545 nm generated on dielectric substrate to the electric field x component. Figure 5 (b) represents magnetic dipole at 545 nm generated on dielectric substrate to the magnetic field z component.

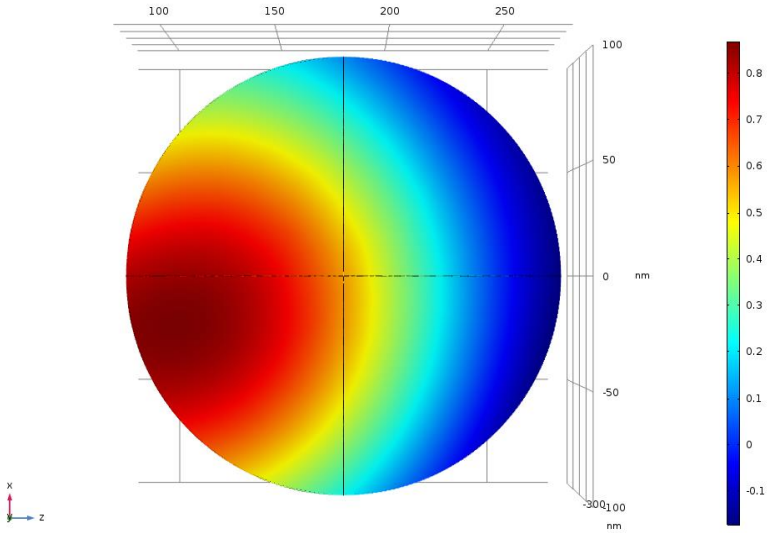

a

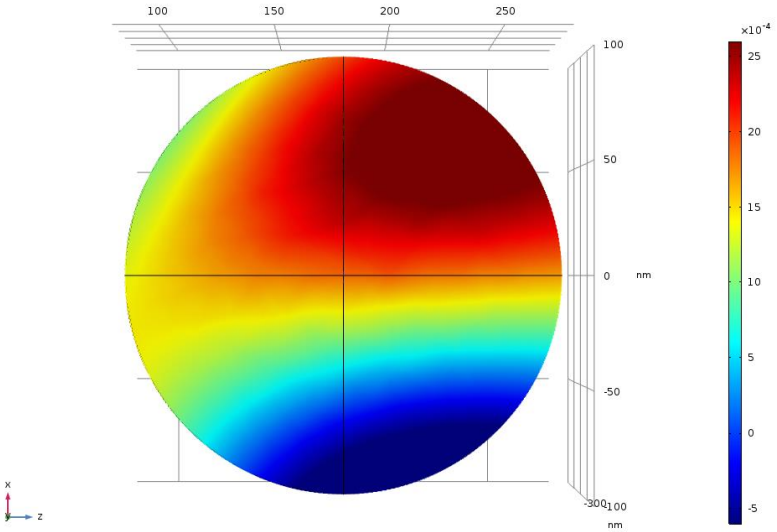

b

Figure 6 (a) represents electric dipole at 720 nm generated on dielectric substrate to the electric field x component. Figure 6 (b) represents magnetic dipole at 720 nm generated on dielectric substrate to the magnetic field z component.

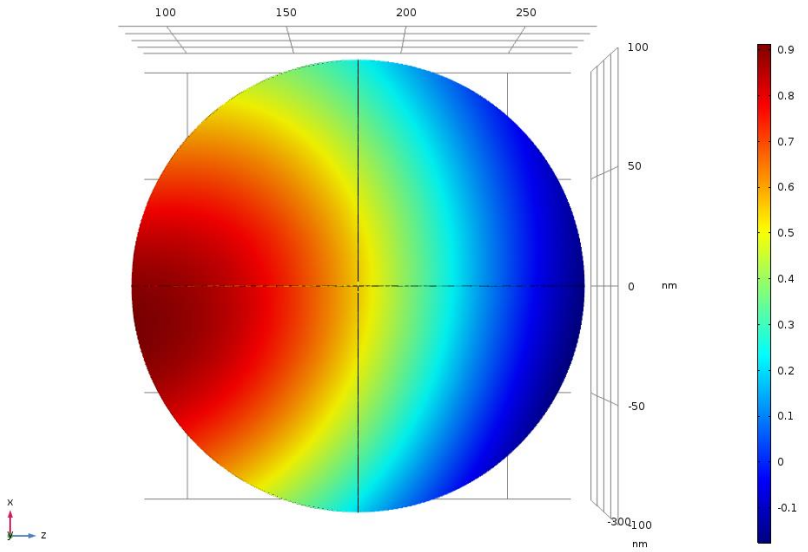

a

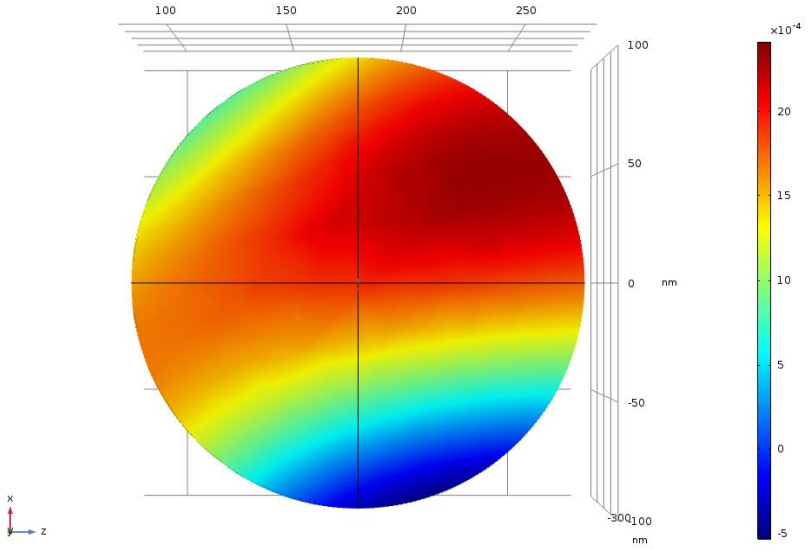

b

Figure 7 (a) represents electric dipole at 780 nm generated on dielectric substrate to the electric field x component. Figure 7 (b) represents magnetic dipole at 780 nm generated on dielectric substrate to the magnetic field z component.

For chiral particle on dielectric substrate, we obtain Optical pulling force from the range of wavelength 535 nm to 570 nm and 650 nm to 1200 nm. The highest optical pulling force is achieved at the range of 700 nm to 800 nm wavelength.

From the simulation we find, at 545 nm wavelength, an electric dipole is created to the y component on dielectric substrate. At the same wavelength a magnetic dipole is also created to the z component.

Considering wavelength 720 nm the chiral particle obtains electric dipole to the y axis and magnetic dipole to the z axis. The same phenomena are observed at 780 nm of chiral particle on dielectric substrate, electric dipole and magnetic dipole is created to the y and z axis accordingly. Notice that, at these ranges the chiral particle is achieving optical pulling force. Certainly, cross product of electric dipole to the y component and magnetic dipole to the z component can be the reason for recoil force to the x component. Equation number (5) verifies our finding. The recoil force is dominant and thus it leads to obtaining Optical pulling force.

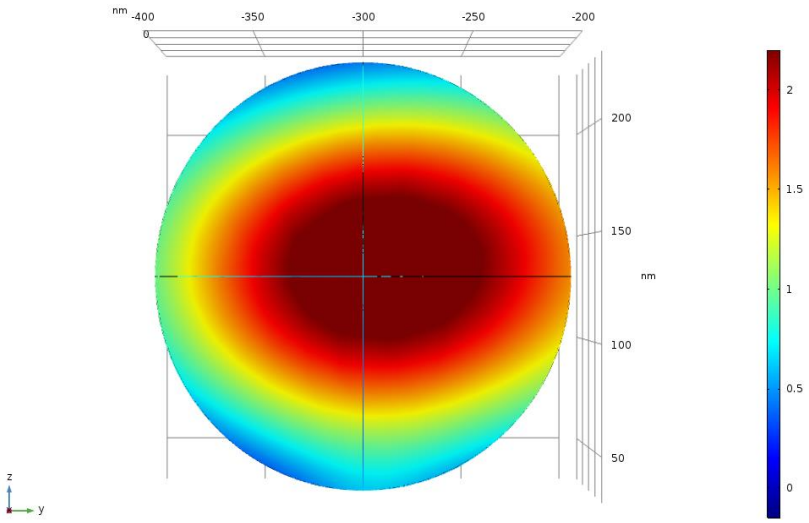

a

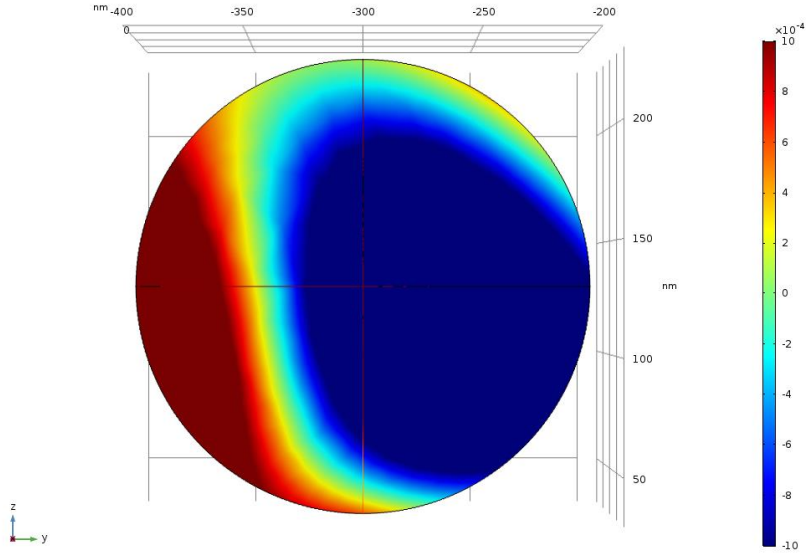

b

Figure 8 (a) represents electric single pole at 545 nm generated on pec substrate to the electric field y component. Figure 8 (b) represents magnetic dipole at 545 nm generated on pec substrate to the magnetic field z component.

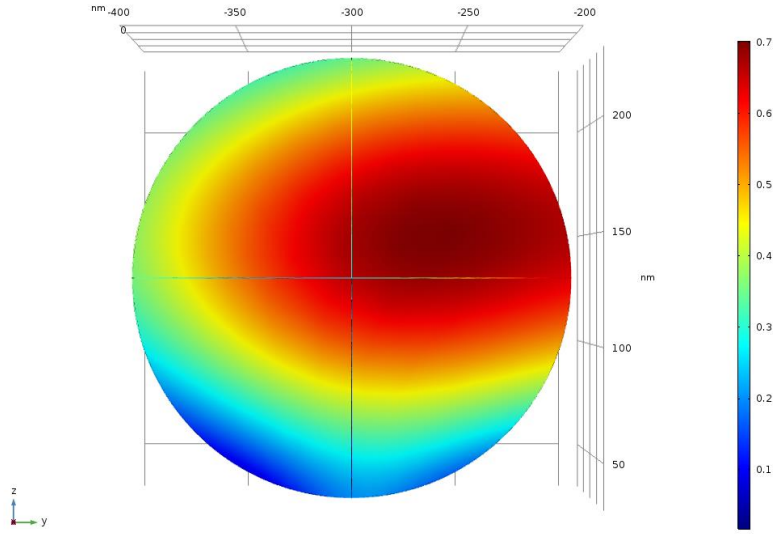

a

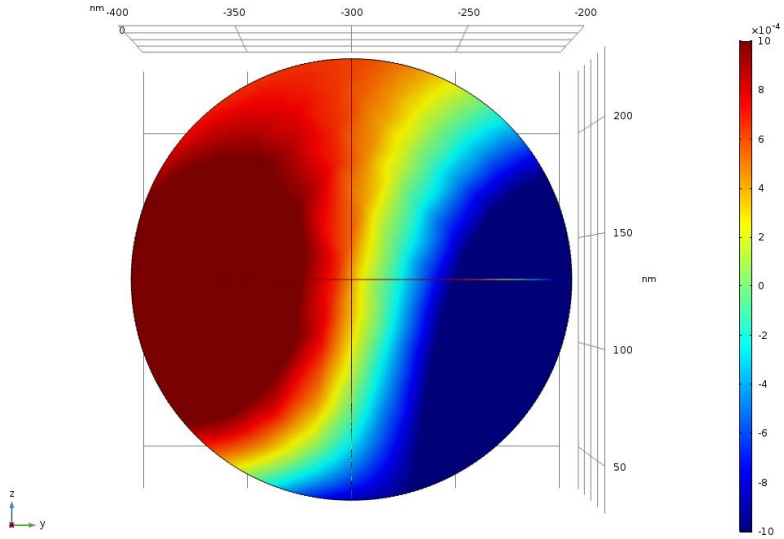

b

Figure 9 (a) represents electric single pole at 720 nm generated on pec substrate to the electric field y component. Figure 9 (b) represents magnetic dipole at 720 nm generated on pec substrate to the magnetic field z component.

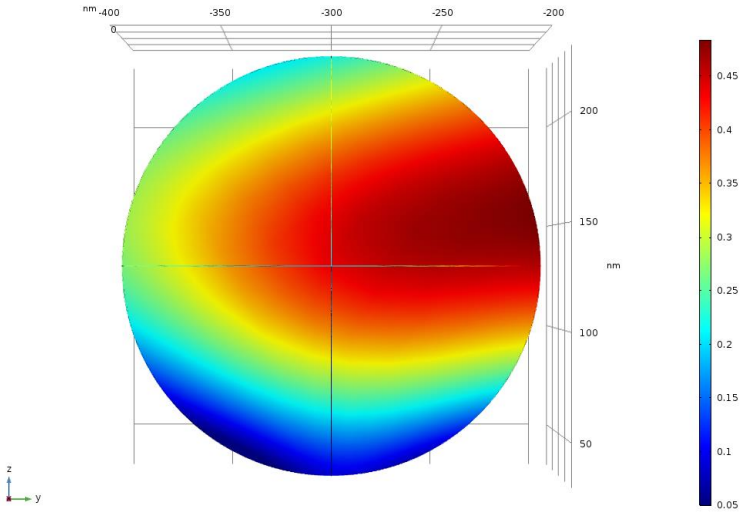

a

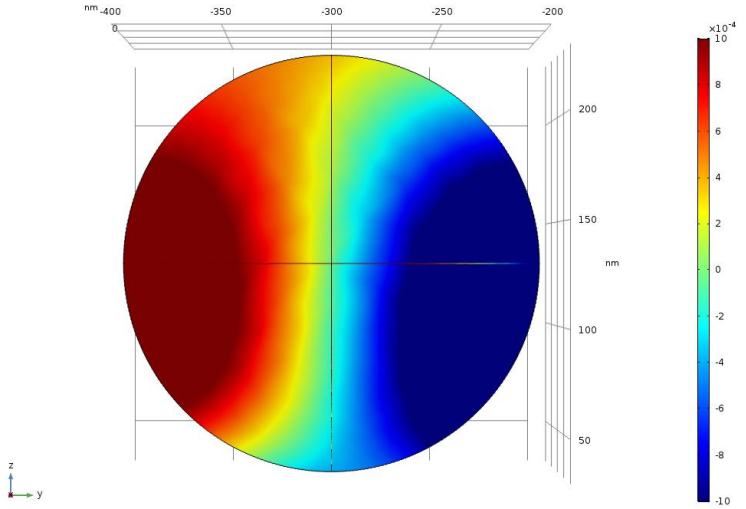

b

Figure 10 (a) represents electric and single pole at 780 nm generated on pec substrate to the electric field y component. Figure 10 (b) represents magnetic single pole at 780 nm generated on pec substrate to the magnetic field z component.

To compare, we are replacing dielectric substrate with plasmonic substrate. At 545 nm of wavelength the chiral particle on plasmonic substrate obtains optical pushing force. So, from the simulation, we see an electric single pole are created to the y component and a magnetic dipole to the z component. The wavelength 720 nm shows indistinguishable consequence. A single

electric pole to the y axis and a magnetic dipole to the z axis are created here on plasmonic substrate. In contrast, at the wavelength 780 nm, a single electric pole and a single magnetic pole are created to the y and z axis accordingly. Here, we achieve optical pulling force form the range of wavelength 1115 nm to 1200 nm. So, acquiring cross product of electric dipole and magnetic dipole is not possible. Recoil force becomes recessive and dominant to extinction cross section force. So, an optical pushing force appears rather than pulling force which we saw to happen earlier on dielectric substrate.

To have an alternate approach we are summing up all three equations after some mathematical computation, [3]

$$\langle F\rangle = -\nabla\langle U_f\rangle + \frac{1}{4}Re\begin{Bmatrix} T^{ee}:\vec{\alpha}^{ee} + T^{em}:\vec{\alpha}^{em} \\ +T^{mm}:\vec{\alpha}^{mm} + T^{me}:\vec{\alpha}^{emT}\end{Bmatrix} - \frac{k^4}{12\pi\epsilon_0 c}Re\left(\tilde{L}+\widetilde{S}\right) \qquad (06)$$

where $\langle f\rangle$ denotes the time averaged value of

$$\langle U_f\rangle = -Re(\alpha_{ee})\frac{\langle U_e\rangle}{\varepsilon_0} - \mu_0 Re(\alpha_{mm})\langle U_m\rangle - Im(\alpha_{em})\frac{K_{chirality}}{\varepsilon_0\omega}$$

is a scalar which can be interpreted as the time averaged free energy, and

$$\langle \mathrm{U_e}\rangle = \varepsilon_0|\mathrm{H}|^2/4$$
$$\langle \mathrm{U_m}\rangle = \mu_0|\mathrm{H}|^2/4$$

are the electric and magnetic energy density.

To understand better chirality induced optical force, equation (6) can be simplified to [4]

$$\begin{aligned}\langle F\rangle = -\nabla\langle U_f\rangle + (C_{ext} + C_{recoil})c^{-1} + \langle S\rangle + \nabla\times[C_{ext}^{p}c\,\langle L_s^p\rangle + C_{ext}^{m}c\,\langle L_s^m\rangle \\ + \mu_0(Re\alpha_{em})\langle S\rangle] + [2\omega^2\mu_0(Re\alpha_{em}) - \frac{k^5}{3\pi\epsilon_0}\frac{Im(\alpha_{ee}{\alpha_{mm}}^*)}{\epsilon_0}]\langle L_s^p\rangle \\ + [2\omega^2\mu_0(Re\alpha_{em}) - \frac{k^5}{3\pi\epsilon_0}Im(\alpha_{mm}{\alpha_{em}}^*)]\langle L_s^m\rangle\end{aligned} \qquad (07)$$

Here,

$$\langle L_s^p \rangle = \frac{\mu_0}{4\omega i} H \times H^*$$

$$\langle L_s^m \rangle = \frac{\epsilon_0}{4\omega i} E \times E^*$$

Where,

$$C_{ext} = C_{ext}^p + C_{ext}^m$$

is the extinction cross section, and

$$C_{ext}^p = \frac{kIm(\alpha_{ee})}{\epsilon_0}$$

$$C_{ext}^m = k\mu_0 Im(\alpha_{mm})$$

are, respectively, the part of extinction coefficient caused by the electric and magnetic dipoles.

$$C_{recoil} = \frac{-k^4 \mu_0}{6\pi\epsilon_0} [Re(\alpha_{ee}\alpha_{mm}{}^*) + |\alpha_{em}|^2]$$

is directly related to the recoil force.

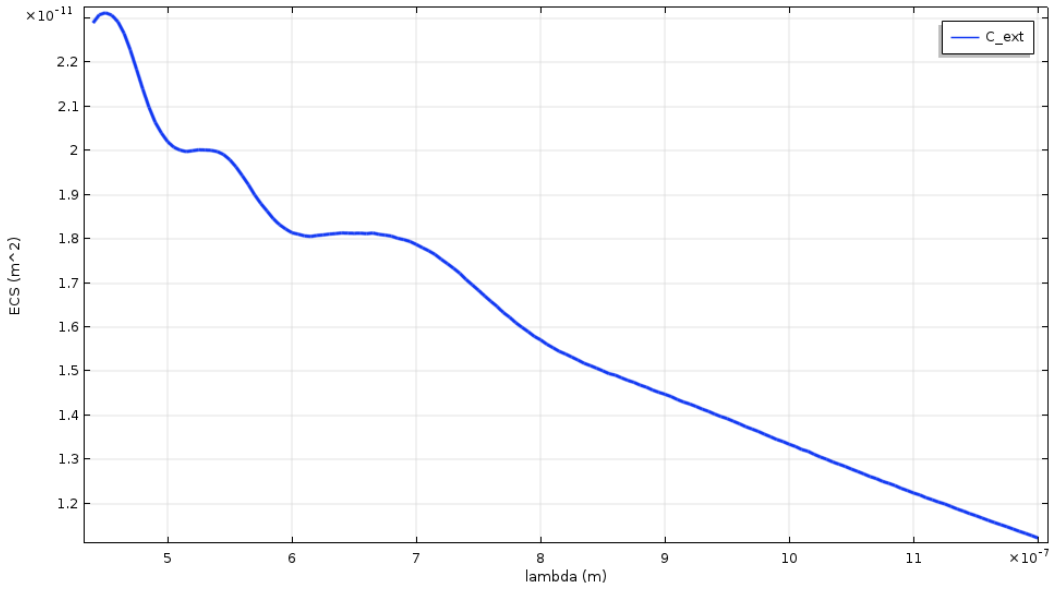

Figure 11 (a) represents the C_{ext} (extinction cross section) on dielectric substrate. With the increase of wavelength, force C_{ext} is starts decreasing. C_{ext} remains high till 600 nm. After 680 nm it keeps degrading.

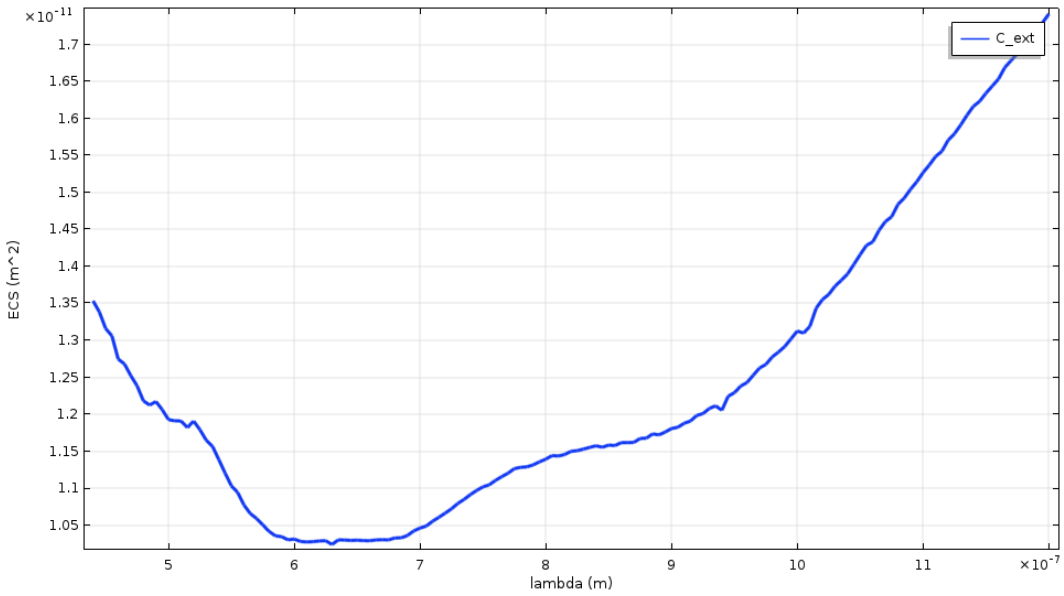

Figure 11 (b) represents the C_{ext}(extinction cross section) force on plasmonic substrate. With the increase of wavelength, force C_{ext} is starts increasing. C_{ext} is the lowest from 600 nm to 700 nm. The force start increasing after 700 nm.

The graph 11(a) is plotted on dielectric substrate. The relation between C_{ext} (extinction cross section) and wavelength range are followed. The C_{ext} is higher till the wavelength of 600 nm. But it starts decreasing after 680 nm. As C_{ext} is the positive force from equation (7), the negative recoil force, C_{recoil} will dominate the extinction cross section C_{ext} .

The graph 11 (b) is plotted on plasmonic substrate. The C_{ext} force is lower till the wavelength of 700 nm. But it starts increasing after 700 nm. C_{ext} (extinction cross section) increased value leads to the domination over recoil force, C_{recoil}.

The strong magnetic dipole resonance caused by the coupling of incoming light to the electric field's circular displacement current induces field penetration and phase retardation inside the particle. When the wavelength inside a particle becomes similar to its spatial dimension, or when $2R \approx \lambda/n$, where n is the refractive index of nanoparticle material, R is the nanoparticle radius and λ is the light's wavelength, magnetic resonance occurs.

The nanoparticle must have a relatively large refractive index to have resonances in the visible and infrared (IR) spectral bands for a good quantity of magnetic resonance. The magnetic dipole mode of a chiral nanoparticle was activated by magnetic resonance at the wavelength of the pulling range. Magnetic resonance has a significant boost to scattering efficiency, as can be seen. The electric and magnetic dipoles are excited perpendicular to one other along the relevant incident field components, and when this falls on a chiral nano-particle, it creates multipoles (in our configuration, quadrupoles), which are the reason for negative scattering force [63].

By utilizing the magnetic resonance modes of the particle, the spin-orbit coupling of the magnetic-field components of light provides a recoil optical force on particles [64]. The recoil force in the chiral particle is induced by the magnetic field in the particle, which can be modified by tuning the chirality of the incident light. Additionally, the induced recoil force can be affected by the magnetic resonance modes of the particle, such as the magnetic-dipole and quadrupole modes, and the recoil force can be enhanced by the magnetic-field resonances in the particle. The larger the magnetic resonance field, the more likely the chiral particle will experience a substantial quantity of induced recoil force [65].

Magnetic resonance was first observed in our simulation at 650 nm (pulling range). We discovered a link between magnetic resonance and recoil force in our system. Magnetic resonance is seen in the pulling range but not in the pushing range of the chiral particle in our setup. The current density follows a circular path on pulling range which is missing on pushing range.

As a result, we can argue that magnetic resonance affects chiral pulling or recoil force. We found almost strong magnetic resonance in our experimental graph; thus, we can say that we can acquire recoil force or pulling force through this resonance. As we approach the pulling range, strong magnetic resonance will be the cause of recoil force, which will dominate the overall force and lead to the negative force, also known as pulling force or negative optical pulling force.

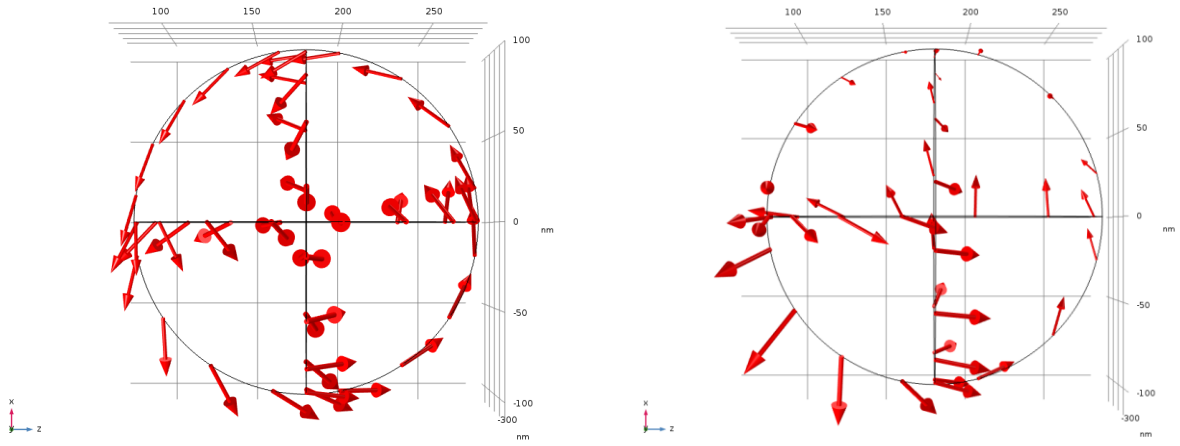

a b

Figure 12 (a) represents the magnetic resonance of chiral particle at 650 nm on dielectric substrate when optical pulling force is in exertion. In figure 12 (b) we don't get any magnetic resonance at 450 nm on dielectric substrate when optical pushing force is in exertion.

CHAPTER-5
PLASMONIC PARTICLE

Plasmonic nanoparticles have electron density that couple with electromagnetic radiation of the wavelength, and they are potent absorbers and scatters of light. The optical response can be adjusted from UV to the visible near the cardinal area of the electromagnetic spectrum by changing their size, shape, and configuration [66]. They are far more significant than the particle due to the nature of the dielectric metal interface [67]. Materials similarly Ag, Cu, Au, and Ai with a negative real and small positive dielectric over a range of wavelengths can support surface plasmon resonance. They can be propagated or localized [68]. An observable effect is seen in the plasmonic nanoparticles, which are called the plasmonic effect. The plasmonic effect can be defined with free electrons and incident light. The effect is known as interactivity between free electrons in metal nanoparticles and incident light. The plasmonic effect is found not only in metal nanoparticles but also in bulk. Both are showing the plasmonic effect, but the effect has a significant difference. Metal nanoparticles are showing a higher effect than bulk. The metal nanoparticle can achieve a more significant plasmonic effect because of the large surface area and favorable plasma generation conditions [69]

Plasmonic nanoparticles made of gold and silver display exciting optical properties on the noticeable range for confining the surface plasmon resonance. Plasmonic nanoparticles can be specifically modulated through variation of particle shape and size. Plasmonic coupling between nanoparticles can create electric fields. A Plasmonic material exploits surface plasmon resonance that is not seen in nature and has achieved optical properties [70] Surface plasmon has great use in the optical system. The binding of molecules can be measured by surface plasmon resonance. There is a conduction band electron in surface plasmon resonance. They are collective oscillations of conduction band electrons present in the resonance where electric field and incident light are oscillating, which can manufacture energetic plasmonic electrons. Surface plasmon requires an interface. Hence an evanescent wave is confined to metal and dielectric interface. As a result, surface plasmon in thin-film structure or localized Surface plasmon resonance in nanoparticles are observed [71].

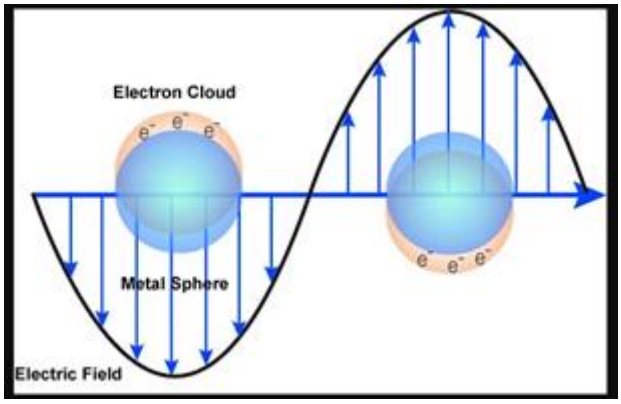

Figure13: Surface plasmon Resonance

A plasmonic nanoparticle can captivate and scatter light more than its own physical size when it is at the maximum resonance. This process can find total loss which is created due to the radiation. The localized surface plasmon resonance dominates spectra of the energy of an optical cross-section of the nanoparticles. Size and shape can play a vital role in this process. They can determine the peak position and the width of the resonance [72] Maxwell's equation can solve a far-field spectrum of a spherically shaped nanoparticle with a harmonic wave equation known as Mie theory [73] A nanoparticle with radius r and a frequency-dependent complex dielectric function $\mathrm{E(w)} = E_1(w) + iE_2(w) = {n_p}^2$ implant in a medium of permittivity $E_m = {\mathrm{n}_m}^2$ and interacting with the light of a wavelength λ_0, the scattering expression $\sigma_{sca}$and extinction cross-section σ_{ext} are [73].

$$\sigma_{sca} = \frac{2\pi R^2}{x^2}\sum_{I=1}^{\infty}(2l+1)\{|{a_1}^2| + |{b_1}^2|\}$$

$$\sigma_{ext} = \frac{2\pi R^2}{x^2}\sum_{I=1}^{\infty}(2l+1)\,Re\,[a_1 + b_1]$$

where $X = \frac{w}{e}n_m = \frac{2\pi}{\lambda_0}n_m$ and c is the speed of light. The absorption cross-section is gained by the difference between the extinction and scattering cross-sections: $\sigma_{abs} = \sigma_{sca} = \sigma_{ext}$. Here a1 and b1 are unknown, but they can be computed from the Riccati-Bessel functions [72].

While using plasmonic nanoparticle (r = 100 nm) on dielectric sub, we have obtained optical pushing force at the range of wavelength 440 nm to 655 nm and 865 nm to 945 nm. Optical

pulling force is obtained at the range of wavelength 670 nm to 860 nm and 950 nm to 1200 nm. The plasmonic nanoparticle offers the highest pulling force at 700 nm to 800 nm.

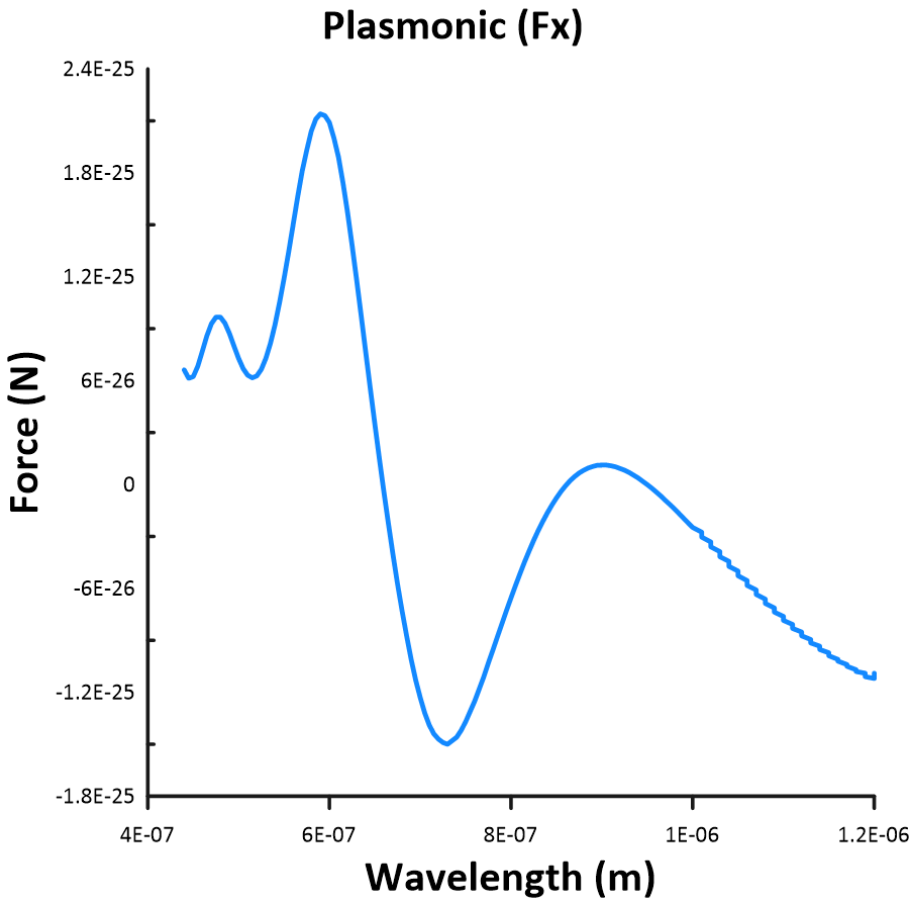

Figure 14 (a) shows the pushing and pulling range of plasmonic nanoparticle on dielectric substrate. The highest pulling range is 700 nm to 800 nm.

While using plasmonic substrate, our experiment experiences an immense contrast. The plasmonic particle displays optical pushing force at the range of wavelength 440 nm to 1200 nm. Our experiment in this context, does not manifest optical pulling force.

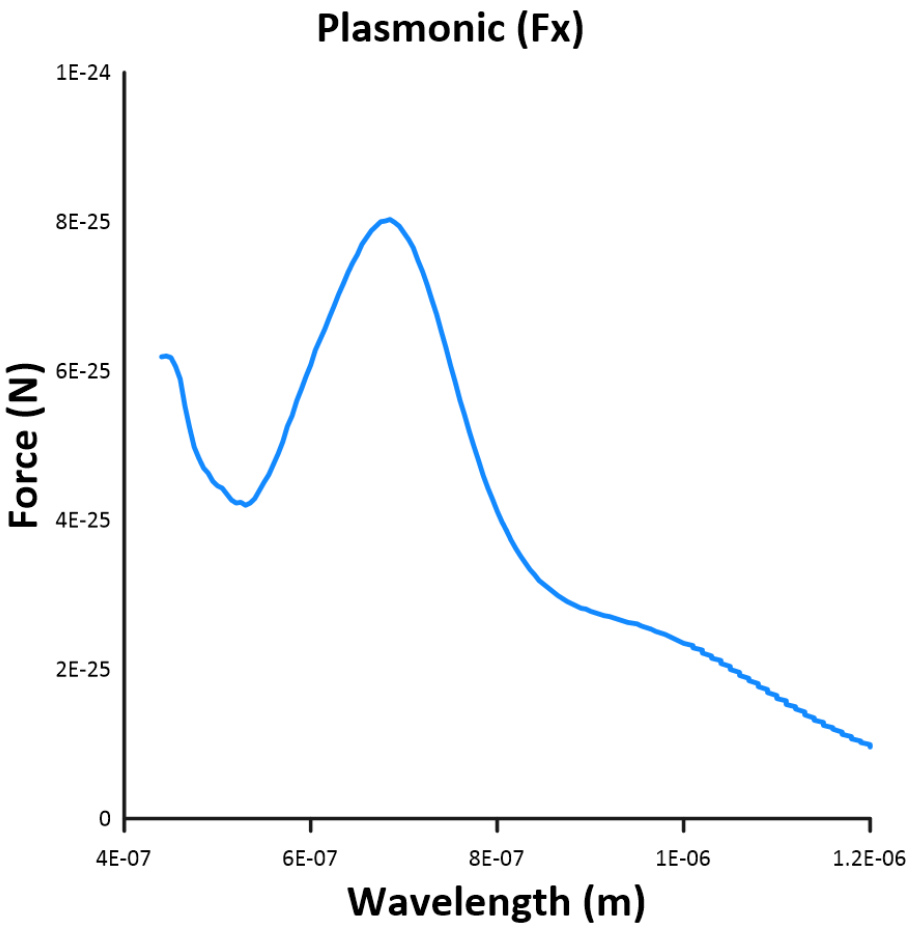

Figure 14 (b) shows the pushing range of plasmonic nanoparticle on plasmonic substrate. The highest pushing range is 650 nm to 750 nm. There's no demonstration of optical pulling force.

In a lossy medium, the optical momentum transfer can be calculated in the same framework of macroscopic electromagnetic theory. To calculate the radiation pressure on an object, the more fundamental way is to utilize Lorentz force. We are applying Lorentz force to bound and free currents and charges. The momentum contribution can be separated into force Fb (bound current and charges) and Fc (free currents). It provides a perception into the procedure of momentum transfer into a lossy media. To explain relevant experimental data and calculate the radiation pressure on absorbing Mie particles, the Lorentz force density and momentum conservation are used interchangeably. As opposed to the scattering and absorption forces estimated for small particles due to the balance between scattering and absorption, we predict that absorption can diminish the total optical momentum transfer to certain particles. The possibility of observing pushing and pulling force enhances. The Lorentz force is applicable directly with complex permittivity $\epsilon = \epsilon_{\mathrm{R}} + i\epsilon_I$ and $\mu = \mu_{\mathrm{R}} + i\mu_I$ in a lossy media [74].

The total time average force $\bar{\mathrm{F}} = \bar{\mathrm{F}}_{\mathrm{b}} + \bar{\mathrm{F}}_{\mathrm{c}}$ can be obtained by doing ingratiation of the time average force densities over the medium. By separation contributed momentum into two parts we can write: [75]

$$\bar{f}_b = \frac{1}{2} Re\{\varepsilon_o(\nabla \cdot \bar{E}) \bar{E}^* + \mu_0(\nabla \cdot \bar{H}) \bar{H}^* - i\omega(\epsilon_R - \epsilon_0)\bar{E} \times \bar{B}^* + i\omega(\mu_R - \mu_0)\bar{H} \times \bar{D}^*\} \quad (08)$$

$$\bar{f}_c = \frac{1}{2} Re\{\omega\epsilon_I \bar{E} \times \bar{B}^* - \omega\mu_I \bar{H} \times \bar{D}^*\} \quad (09)$$

$(*)$ is the complex conjugate. ϵ_R (ϵ_I) is the real (imaginary) part of the relative permittivity.

In a lossy system, the force density on the bound electric charges and currents fb can be positive or negative depending on the polarization P at that position [75]. The force density on free currents fc is a pushing force because the incident light contracts and transfers momentum. The pulling force can be enhanced due to the dominant negative Lorentz force on bound currents and charges [75].

To connect the equation (8) and (9) with momentum conservation, let us consider an electromagnetic wave with complex wave number $\mathrm{K_x}$ where $\mathrm{K_x} = \mathrm{K_{xR}} + \mathrm{iK_{xI}}$. we get,

$$\bar{f}_b = -\hat{x}\frac{1}{2} K_{xI}[(\epsilon_R - \epsilon_0) |\bar{E}|^2 + (\mu_R - \mu_0) |\bar{H}|^2] \quad (10)$$

$$\bar{f}_c = \hat{x}\frac{1}{2} K_{xR}[\epsilon_I |\bar{E}|^2 + \mu_I |\bar{H}|^2] \quad (11)$$

Here, H is the magnetic field. When the medium is optically dense, the force on the bound currents is opposite to the incident wave propagation direction, as indicated by the negative sign leading the left-hand side of equation (10)

Force density on free currents is:

$$\bar{f}_c = \hat{x}\frac{1}{2}\frac{n\omega}{c}[\epsilon_I |\bar{E}|^2 + \mu_I |\bar{H}|^2] = -\hat{x}\frac{1}{2} Re\left\{\frac{n}{c} \nabla \cdot \bar{S}\right\} \quad (12)$$

Where $n = \frac{ck_{zR}}{\omega}$ is the index of refraction, c is the speed of light in vacuum, and $\bar{S} = \bar{E} \times \bar{\mathrm{H}}^*$ is the complex Poynting vector resulting from the application of Pointing's theorem to the second equality.

In our experiment, on dielectric substrate, plasmonic particle show optical pushing force at the wavelength 545 nm. The optical pulling force is obtained at the wavelength of 800 nm. From the simulation we find, at 545 nm on dielectric substrate, the arrow lines of current density are dominant to the ''+x'' axis meaning the polarization is in the same plane of light. So, the plasmonic particle manifests pushing force. At the wavelength of 800 nm on dielectric particle, the current density is dominant to the opposite direction of light propagation. As from the simulation we can see, the arrow lines of the current density are dominant to the ''-x'' axis. So here on plasmonic particle, we have obtained optical pulling force. So, the observation is, in optical pulling and pushing range, the pole reversal occurs frequently.

From figure (3) the quadrupole configuration of optical pushing force at 475 nm is altering at 800 nm when optical pulling force is occurring. We have observed, with the change of optical pulling and pushing force, the phase reversal occurs frequently.

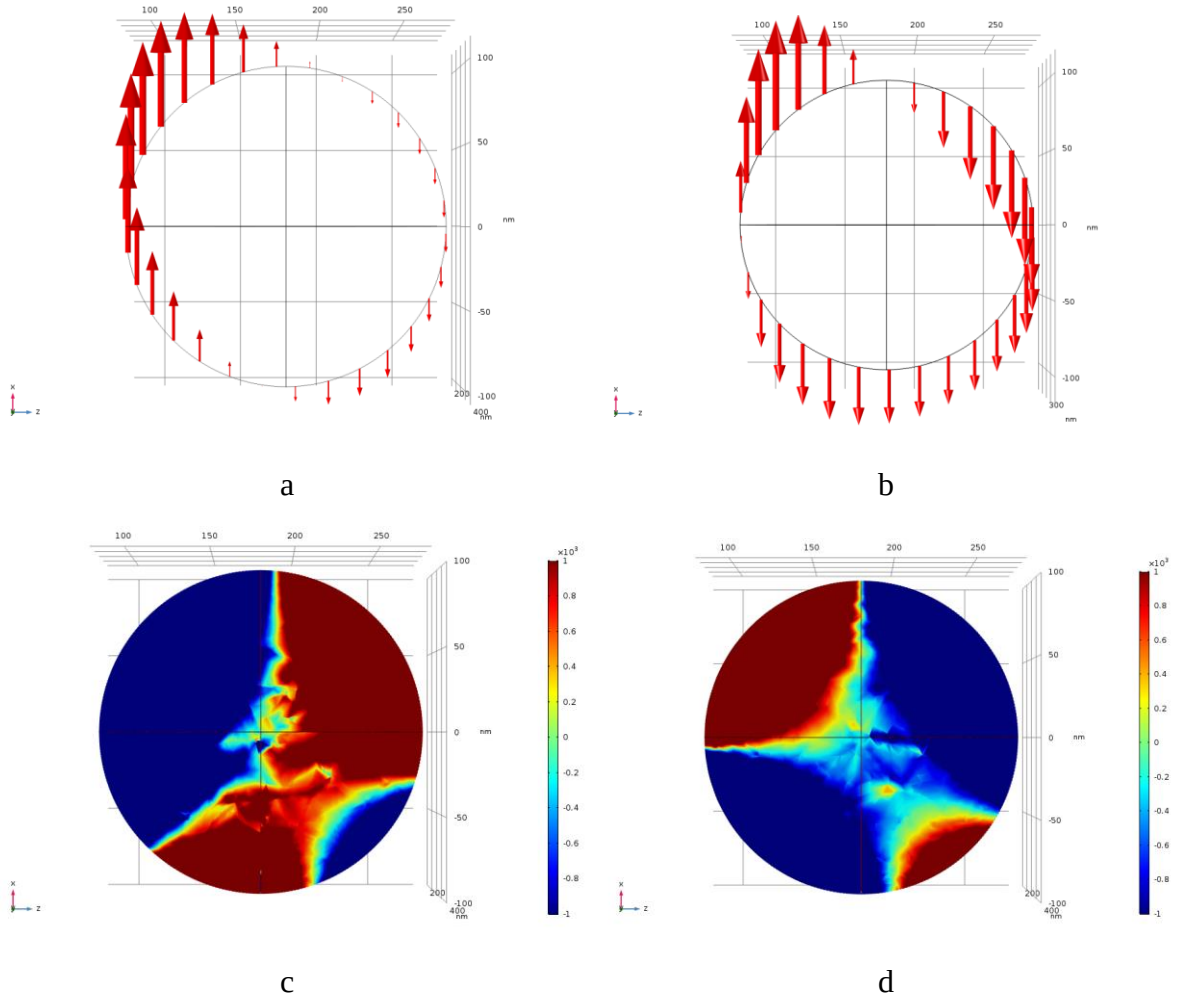

a b c d

Figure 15 (a) and (b) represents the arrow lines of charge density on dielectric substrate for plasmonic particle at 545 nm and 800 nm wavelength. In figure 15 (a) the dominant arrow lines of current density

are polarized to the same direction as optic polarization. Figure 15 (b) shows that the dominant arrow lines of current density are in the opposite direction of optic polarization. Figure 15 (c) and (d) presents the phase reversal of current density at 475 nm and 800 nm.

To strengthen our position, we are comparing the concept with plasmonic substrate. Astonishingly, the plasmonic nano particle on the plasmonic substrate never obtains optical pulling force. At the both wavelengths of 545 nm and 800 nm, only optical pushing force is displayed. From the simulation, it can be said, the current density at 545 nm is dominant to the same plane as the polarization of light (+x axis). also, at 800 nm the behavior is the same. The current density is dominant to ''+x'' axis. We have observed that, at 545 nm on dielectric substrate, the particle shows optical pushing force and the polarization is towards ''+x'' axis. So, the similarity of phase of current density on both substrates for the pushing range is noticeable.

From figure 16 (c) we observe a quadrupole at 800 nm where pushing force is obtained. So, both on dielectric and plasmonic substrate we get the same configuration of quadrupole when the particle reveals optical pushing force.

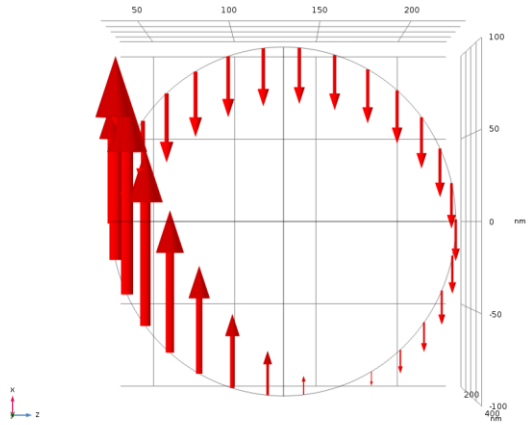

a

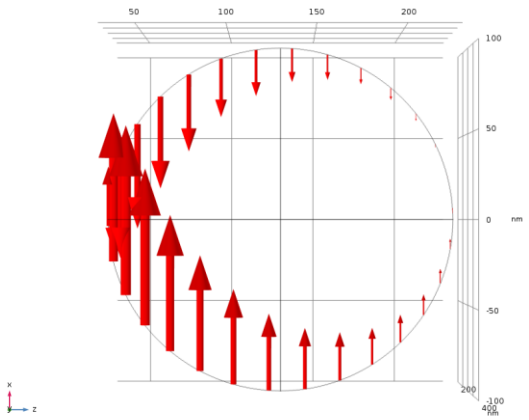

b

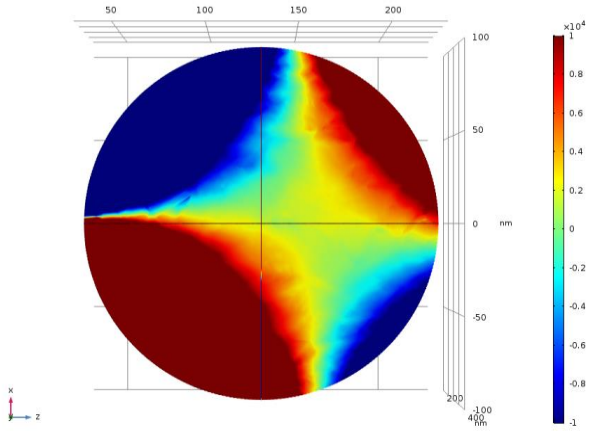

c

Figure 16 (a) and (b) represents the arrow lines of charge density on the plasmonic substrate for plasmonic particle at 545 nm and 800 nm wavelength. The dominant arrow lines of current density here are polarized to the same direction as optic polarization. Figure 16 (c) presents a quadrupole configuration of current density at 800 nm which is similar to fig 15 (c).

CHAPTER-6
RESULT AND DISCUSSION

In our set up, our aim was to observe the behavior of three nano particles (chiral, dielectric and plasmonic) of the same radius (r = 100 nm). For that, we have used two substrates: dielectric and plasmonic. The experiment shows how the particles behave differently when the substrate is changed. The range of wavelength for the experiment was taken from 440 nm to 1200 nm. The emergence of optical pulling and pushing force for all three nanoparticles was observable. Astonishingly, we have achieved the highest optical pulling force for the three nano particles at 700 nm to 800 nm range on dielectric substrate. On the other hand, we have gotten an optical pushing force at the same range of 700 to 800 nm on plasmonic substrate.

Noticeably, we are using a particle that is smaller than the wavelength. For dielectric and chiral nanoparticles, we have used Minkowski stress tensor to explain the optical pulling force. But for plasmonic particle Lorentz force was more applicable to understand.

From figure (3) In dielectric particle, the interference of electric dipole and quadrupole results in optical pulling force on dielectric substrate. While using a plasmonic substrate, optical pushing force is obtained when an electric dipole occurs. We also get optical pulling force on plasmonic substrate at 1000 nm and it has the similar reason as dielectric substrate, interference of electric dipole and quadrupole.

In plasmonic particle, current density plays a big role to obtain pulling and pushing force. From figure (15) In plasmonic particle, we have found reversal of current density and phase. On dielectric substrate, the reversal of current density results in optical pulling force. However, on the plasmonic substrate we don't see any reversal of current density. The phase is exactly same as the plasmonic particle on dielectric substrate for optical pushing force.

We observe the emergence of recoil force in chiral particle. On dielectric substrate, the pulling force occurs for the high recoil force. But on plasmonic substrate, the lower recoil force leads in to optical pushing force. From another perspective, we get magnetic resonance at the same range where optical pulling force occurs. The relation between recoil force and magnetic resonance amplifies the possibility of finding optical pulling force. On the contrary, plasmonic substrate does not show any magnetic resonance. So, we see the absence of optical pulling force at the range.

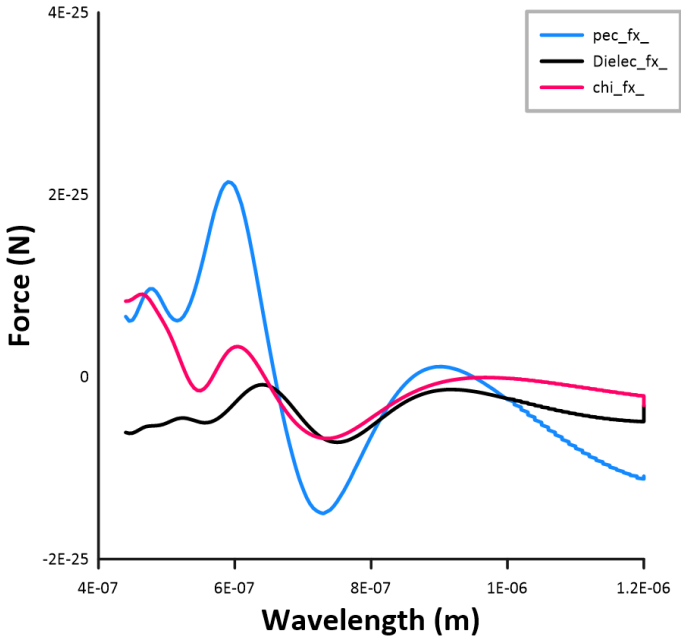

Figure 17 (a) shows the pushing and pulling range of plasmonic, dielectric and chiral nanoparticles on a dielectric substrate. Between 700 nm to 800 nm wavelength all three particles show pulling force and it's the highest pulling range.

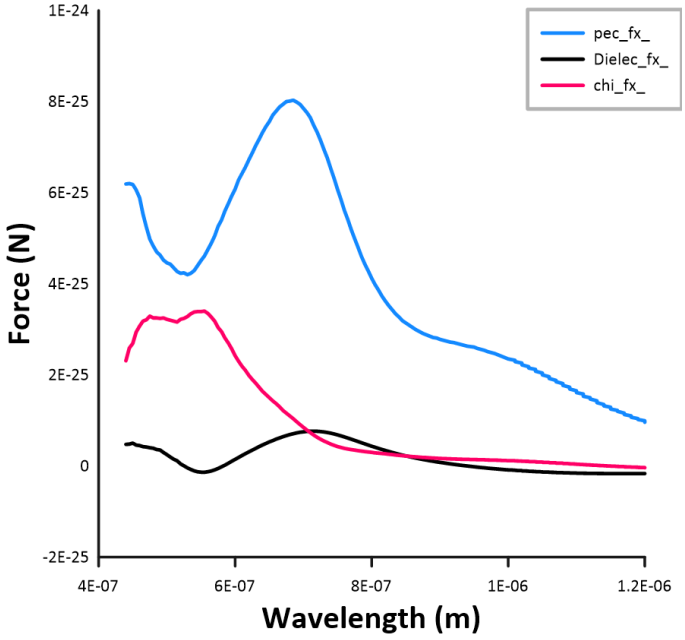

Figure 17 (b) shows the pushing and pulling range of plasmonic, dielectric and chiral nanoparticles on a plasmonic substrate. Between 700 nm to 800 nm wavelength all three particles show pushing force.

CHAPTER-7
CONCLUSION

In this letter, we have provided a perspective of optical pulling force in chiral, dielectric and plasmonic nanoparticles. The method explained here is basically for Rayleigh particles (particle size is smaller than wavelength) and it satisfies all three nanoparticles. However, the approach has to be changed for larger particles. In this experiment, the predicted optical force by the analytical theory is demonstrated by applying Minkowski stress tensor and Lorentz force. Optical pulling force on dielectric and chiral particles were proven by mie scattering theory and Minkowski stress tensor but for plasmonic particle we explained the optical pulling force by Lorentz force. Though the total optical force was proven by Minkowski stress tensor. We considered the wavelength range to 440 nm to 1200 nm to calculate optical force but the main focus was at the range of 700 nm to 800 nm as the optical pulling force was highest at this range on dielectric substrate. Not only that, we have also verified, optical pulling force is present for all three nanoparticles at the same range of wavelength for dielectric substrate. But for plasmonic substrate, the same range of wavelengths shows optical pushing force rather than optical pulling force. We have also tried to explain the reason for finding optical pushing force. We have noticed, the behavior of the particles and optical pulling or pushing force get changed when the substrates are altered and the wavelengths are varied. The finding can be a novel way to explore further on optical manipulation. All the simulations here are done by COMSOL Multiphysics 5.3a.

CHAPTER-8
REFERENCES

1. Jona´s and P. Zem ˇ anek, “Light at work: The use of optical forces for ´ particle manipulation, sorting, and analysis,” Electrophoresis, vol. 29, no. 24, pp. 4813–4851, Dec. 2008.
2. Pavel Zemánek, Giorgio Volpe, Alexandr Jonáš, and Oto Brzobohatý, "Perspective on light-induced transport of particles: from optical forces to phoretic motion," Adv. Opt. Photon. 11, 577-678 (2019).
3. Hang Li, Yongyin Cao, Lei-Ming Zhou, Xiaohao Xu, Tongtong Zhu, Yuzhi Shi, Cheng-Wei Qiu, and Weiqiang Ding, "Optical pulling forces and their applications," Adv. Opt. Photon. 12, 288-366 2020.
4. Realization of optical pulling forces using chirality Kun Ding, Jack Ng, Lei Zhou, and C. T. Chan Phys. Rev. A 89, 063825 – Published 27 June 2014.
5. Ashkin, A., Dziedzic, J. M., & Yamane, T. (1987). Optical trapping and manipulation of single cells using infrared laser beams. Nature, 330(6150), 769.
6. Gao, D., Ding, W., Nieto-Vesperinas, M., Ding, X., Rahman, M., Zhang, T., ... & Qiu, C. W. (2017). Optical manipulation from the microscale to the nanoscale: fundamentals, advances and prospects. Light: Science & Applications, 6(9), e17039-e17039.
7. D. M. Lipkin, J. Math. Phys. 5, 696 (1964).
8. Chen, J., Ng, J., Lin, Z., and Chan, C. T., “Optical pulling force”, Nature Photonics, vol. 5, no. 9, pp. 531–534, 2011. doi:10.1038/nphoton.2011.153.
9. P. L. Marston, “Axial radiation force of a Bessel beam on a sphere and direction reversal of the force,” J. Acoust. Soc. Am. 120, 3518–3524 (2006).
10. W. Ding, T. Zhu, L.-M. Zhou, and C.-W. Qiu, “Photonic tractor beams: a review,” Adv. Photon. 1, 024001 (2019).
11. M. Mansuripur, “Comment on ‘observation of a push force on the end face of a nanometer silica filament exerted by outgoing light’,” Phys. Rev. Lett. 103, 019301 (2009).
12. S. M. Barnett, “Resolution of the Abraham-Minkowski dilemma,” Phys. Rev. Lett. 104, 070401 (2010).
13. P. W. Milonni and R. W. Boyd, “Momentum of light in a dielectric medium,” Adv. Opt. Photon. 2, 519–553 (2010).
14. . C. Garrison and R. Y. Chiao, “Canonical and kinetic forms of the electromagnetic momentum in an ad hoc quantization scheme for a dispersive dielectric,” Phys. Rev. A 70, 053826 (2004).
15. C.-W. Qiu, W. Ding, M. R. C. Mahdy, D. Gao, T. Zhang, F. C. Cheong, A. Dogariu, Z. Wang, and C. T. Lim, “Photon momentum transfer in inhomogeneous dielectric mixtures and induced tractor beams,” Light Sci. Appl. 4, e278 (2015).

16. O. Brzobohatý, V. Karásek, M. Šiler, L. Chvátal, T. Cižmár, and P. Zemánek, ˇ “Experimental demonstration of optical transport, sorting and self-arrangement using a ‘tractor beam,’” Nat. Photonics 7, 123–127 (2013).
17. J. Chan et al., “Laser cooling of a nanomechanical oscillator into its quantum ground state,” Nature 478, 89–92 (2011).
18. C. H. Metzger, “Cavity cooling of a microlever,” Nature 432, 1002–1005 (2004).
19. A Schliesser et al., “Resolved-sideband cooling and position measurement of a micromechanical oscillator close to the Heisenberg uncertainty limit,” Nat. Phys. 5, 509–514 (2009).
20. N. Descharmes et al., “Observation of backaction and selfinduced trapping in a planar hollow photonic crystal cavity,” Phys. Rev. Lett. 110(12), 123601 (2013).
21. M. Righini et al., “Surface plasmon optical tweezers: tunable optical manipulation in the femtonewton range,” Phys. Rev. Lett. 100(18), 186804 (2008).
22. M. L. Juan et al., “Self-induced back-action optical trapping of dielectric nanoparticles,” Nat. Phys. 5(12), 915–919 (2009).
23. S. Sukhov and A. Dogariu, “Non-conservative optical forces,” Rep. Progr. Phys. 80(11), 112001 (2017).
24. C. Zensen et al., “Pushing nanoparticles with light—a femtonewton resolved measurement of optical scattering forces,” APL Photonics 1(2), 026102 (2016).
25. M R C Mahdy, Hamim Mahmud Rivy, Ziaur Rahman Jony, Nabila Binte Alam, Nabila Masud, Golam Dastegir Al Quaderi, Ibraheem Muhammad Moosa, Chowdhury Mofizur Rahman, M Sohel Rahman Dielectric or plasmonic Mie object at air-liquid interface: The transferred and the traveling momenta of photon 2020 Chin. Phys. B 29 014211.
26. Fantastic quasi-photon and the symmetries of Maxwell electromagnetic theory, momentum-energy conservation law, and Fermat's principle, Optik, Volume 172, 2018, Pages 1211-1217, ISSN 0030-4026.
27. Anne Lisa Wolf, Jonas Morgenweg, Jeroen C. J. Koelemeij, Steven A. van den Berg, Wim Ubachs, and Kjeld S. E. Eikema, "Direct frequency-comb spectroscopy of a dipole-forbidden clock transition in trapped Ca+40 ions," Opt. Lett. 36, 49-51 (2011).
28. Erratum: Colloquium: Momentum of an electromagnetic wave in dielectric media [Rev. Mod. Phys. 79, 1197 (2007)] Robert N. C. Pfeifer, Timo A. Nieminen, Norman R. Heckenberg, and Halina Rubinsztein-Dunlop Rev. Mod. Phys. 81, 443 (2009).
29. Observation of a Push Force on the End Face of a Nanometer Silica Filament Exerted by Outgoing Light Weilong She, Jianhui Yu, and Raohui Feng Phys. Rev. Lett. 101, 243601 (2008)’.
30. Optical trapping and manipulation of neutral particles using lasers Arthur Ashkin Proceedings of the National Academy of Sciences May 1997, 94 (10) 4853-4860; DOI: 10.1073/pnas.94.10.4853.

31. Y. Tang and A. E. Cohen, Phys. Rev. Lett. 104, 163901 (2010).
32. K. Y. Bliokh and F. Nori, Phys. Rev. A 83, 021803 (2011).
33. A,Ashkin, J. M. Dziedzic, J. E. Bjorkholm, and Steven Chu, "Observation of a single-beam gradient force optical trap for dielectric particles," Opt. Lett. 11, 288-290 (1986).
34. Ashkin, A. & Dziedzic, J. M. (1987) Science 235, 1517–1520.
35. Ashkin, A., Dziedzic, J. M. & Yamane, T. (1987) Nature (London) 330, 769–771.
36. Varat Intaraprasonk and Shanhui Fan, "Optical pulling force and conveyor belt effect in resonator–waveguide system," Opt. Lett. 38, 3264-3267 (2013).
37. A,Dogariu, S. Sukhov, and J. J. Saenz, Nat. Photonics 7, 24 (2012). 2. S. M. Block, Nature 360, 493 (1992).
38. T. Cizmar, V. Kollarova, Z. Bouchal, and P. Zemanek, New J. Phys. 8, 43 (2006).
39. D. B. Ruffner and D. G. Grier, Phys. Rev. Lett. 109, 163903 (2012).
40. O. Brzobohaty, V. Karasek, M. Siler, L. Chvatal, T. Cizmar, and P. Zemanek, Nat. Photonics 7, 123 (2013).
41. Chiral route to pulling optical forces and left-handed optical torques Antoine Canaguier-Durand* and Cyriaque Genet†.
42. D. Hakobyan and E. Brasselet, Nat. Photon. 8, 610 (2014). [31] M. Nieto-Vesperinas, Opt. Lett. 40, 3021 (2015).
43. M. Nieto-Vesperinas, Opt. Lett. 40, 3021 (2015).
44. Surface plasmon polariton assisted optical pulling force Mihail I. Petrov1, Sergey V. Sukhov1,2,3, Andrey A. Bogdanov1, Alexander S. Shalin1,3,4,∗, and Aristide Dogariu2.
45. J. Chen, J. Ng, Z. F. Lin, and C. T. Chan, Nat. Photon 5, 531 (2011).
46. P. C. Chaumet and M. Nieto-Vesperinas, Opt. Lett. 25, 1065 (2000).
47. S. Albaladejo, M. I. Marques, M. Laroche, and J. J. Saenz, Phys. Rev. Lett. 102, 113602 (2009).
48. Naima Binte Ahsan, Rafia Shamim, M. R. C. Mahdy, Saikat Chandra Das, Hamim Mahmud Rivy, Chaity Islam Dolon, Maruf Hossain, and K. M. Faisal, "Chiral and plasmonic hybrid dimer pair: reversal of both near- and far-field optical binding forces," J. Opt. Soc. Am. B 37, 1273-1282 (2020).
49. Zhang, T., Mahdy, M. R. C., Liu, Y., Teng, J. H., Lim, C. T., Wang, Z., & Qiu, C. W. (2017). All-optical chirality-sensitive sorting via reversible lateral forces in interference fields. ACS nano, 11(4), 4292-4300.
50. Qiu, C. W., Ding, W., Mahdy, M. R. C., Gao, D., Zhang, T., Cheong, F. C., & Lim, C. T. (2015). Photon momentum transfer in inhomogeneous dielectric mixtures and induced tractor beams. Light: Science & Applications, 4(4), e278.
51. Zhu, T., Mahdy, M. R. C., Cao, Y., Lv, H., Sun, F., Jiang, Z., & Ding, W. (2016). Optical pulling using evanescent mode in subwavelength channels. Optics express, 24(16), 18436-18444.
52. Mahdy, M. R. C., Zhang, T., Das, S. C., & Rivy, H. M. (2020). On chip optical tractor beam by surface plasmon polariton. Optics Communications, 125395.
53. Bohren, C. F., & Huffman, D. R. (2008). Absorption and scattering of light by small particles. John Wiley & Sons.

54. Lindell, I. V., Sihvola, A. H., Tretyakov, S. A., & Viitanen, A. J. (1994). Electromagnetic waves in chiral and bi-isotropic media.
55. Lassiter, J. B., McGuire, F., Mock, J. J., Ciracì, C., Hill, R. T., Wiley, B. J., ... & Smith, D. R. (2013). Plasmonic waveguide modes of filmcoupled metallic nanocubes. Nano letters, 13(12), 5866-5872.
56. Thabet Mohamed, Ahmed. (2017). Theoretical analysis for effects of nanoparticles on dielectric characterization of electrical industrial materials. Electrical Engineering. 99. 10.1007/s00202-016-0375-4.
57. A.Dogariu, S. Sukhov, J. Sáenz, Optically induced'negative forces', Nat. Photonics 7 (1) (2013) 24.
58. J. Arlt, K. Dholakia, Generation of high-order Bessel beams by use of an axicon, Opt. Commun. 177 (1–6) (2000) 297–301.
59. J. Turunen, A. Vasara, A.T. Friberg, Holographic generation of diffraction-free beams, Appl. Opt. 27 (19) (1988) 3959–3962.
60. D. McGloin, K. Dholakia, Bessel beams: diffraction in a new light, Contemp. Phys. 46 (1) (2005) 15–28.
61. J. A. Kong, Electromagnetic wave theory (EMW, Cambridge, 2000).
62. M. Nieto-Vesperinas, J. J. Sáenz, R. Gómez-Medina, and L. Chantada, "Optical forces on small magnetodielectric particles," Opt. Express 18, 11428–11443 (2010).
63. Yuri Kivshar and Andrey Miroshnichenko, "Meta-Optics with Mie Resonances," Optics & Photonics News 28(1), 24-31 (2017).
64. Fu Y, Zhang Y, Min C, Fu K, Yuan X. Lateral forces on particles induced by magnetic spin-orbit coupling. Opt Express. 2020 Apr 27;28(9):13116-13124. doi: 10.1364/OE.390214. PMID: 32403792.
65. Oh, S.S., Hess, O. Chiral metamaterials: enhancement and control of optical activity and circular dichroism. Nano Convergence 2, 24 (2015).
66. G. M. Whitesides, B. Grzybowski, Science 2002, 295, 2418 – 2421.
67. S. A. Davis, M. Breulmann, K. H. Rhodes, B. Zhang, S. Mann, Chem. Mater. 2001, 13, 3218 – 3226.
68. Correlated Structure and Optical Property Studies of Plasmonic Nanoparticles. Anne-Isabelle Henry,† Julia M. Bingham,† Emilie Ringe,† Laurence D. Marks,‡ George C. Schatz,† and Richard P. Van Duyne*,†.
69. Thompson, B. C.; Frechet, J. M. J. Angew. Chem., Int. Ed. 2008, 47, 58−7.
70. Hierarchical Assembly of Plasmonic Nanoparticles Cyrille Hamon*[a] and Luis M. Liz-Marz□n*[a, b].
71. Mihail I. Petrov1, Sergey V. Sukhov1,2,3, Andrey A. Bogdanov1, Alexander S. Shalin1,3,4,∗, and Aristide Dogariu2, Laser Photonics Rev. 10, No. 1, 116–122 (2016).
72. Jana Olson,a Sergio Dominguez-Medina, an Anneli Hoggard,a Lin-Yung Wang,a Wei-Shun Chang*a and Stephan Link*ab 14 April 2014.
73. U. Kreibig and M. Vollmer, Optical properties of metal clusters, Springer, Berlin, 1995.

74. Kemp, Brandon & Grzegorczyk, Tomasz & Kong, Jin. (2006). Optical Momentum Transfer to Absorbing Mie Particles. Physical review letters. 97. 133902. 10.1103/PhysRevLett.97.133902.
75. Gao, D. & Shi, Ran & Huang, Yang & Ni, W. & Gao, Lei. (2017). Fano-enhanced pulling and pushing optical force on active plasmonic nanoparticles. Physical Review A. 96. 10.1103/PhysRevA.96.043826.
76. Juan, M. L., Gordon, R., Pang, Y., Eftekhari, F. & Quidant, R., Self-induced backaction optical trapping of dielectric nanoparticles. Nature Phys. 5, 915–919 (2009).